A Study of Zinc Transporter 1 and its Role in Type 3 Haemochromatosis

Liza Parkinson

Supervisors: Dr. Ross Graham
A/Professor Debbie Trinder

Examiners: Dr. Ross Graham
Dr. Jane Allan
A/Professor Robert Mead

This thesis is presented as part of the requirement for the Degree of Bachelor of Science in Molecular Biology with Honours at Murdoch University

TABLE OF CONTENTS

CHAPTER THREE – RESULTS

CHAPTER FOUR – DISCUSSION

DECLARATION

This thesis contains no material which has been accepted for the award of any other degree or diploma in any University and to the best of my knowledge and belief, this thesis contains no material previously published or written by another person, except where due reference has been made.

Signed: _____ (Liza Parkinson)

Dated: _____07/08/2009_____

ACKNOWLEDGEMENTS

First, I would like to thank my supervisors, Dr. Ross Graham and Associate Professor Debbie Trinder, for taking me on as an honours student. In addition I would like to express my gratitude to Associate Professor Robert Mead for his supervisory role and for all his guidance, support and encouragement during my undergraduate degree.

Special acknowledgment to my primary supervisor, Ross Graham, for his patience, guidance and assistance - your support has been overwhelming. To Carly Herbison, thank you for your advice, support and willingness to always help – there was nothing that was ever too much trouble. Thank you, also, to Anita Chua and Roheeth Delima for your advice and encouragement, and, together with Dan Johnstone (University of Newcastle), for providing me with liver tissue.

Thank you to Dr. Jane Allan and all the researchers and students at the Fremantle Hospital Medical Science Lab for their support and friendship.

It would be remiss of me not to acknowledge the many Academics I have encountered during my time at Murdoch University - thank you for your assistance, encouragement and inspiration.

I would also like to thank my family and friends who encouraged and believed in me. Tara, Nicola and Matthew, my beautiful children, thank you for your help but especially for your unconditional love and understanding. To Wayne, thank you

for your help and encouragement. Special thanks to my sister and best friend, Antoinette, who encouraged me to obtain my degree and believed in me when I didn't think I could do it – you are my inspiration. To my mother-in-law, The Late Jeanette Parkinson (Dec.), who often reminded me of my achievements and always told me how proud she was of me - thank you and I wish you were here to see that I made it.

Finally, an enormous expression of gratitude to my wonderful parents, Jerry and Grace Fedele, without whose encouragement and support it would not have been possible for me to undertake this project - I simply could not have done this without you .

I am grateful to the Fremantle Hospital Medical Research Foundation for partial funding of this research.

LIST OF FIGURES

LIST OF TABLES

ABBREVIATIONS

BCP	1-Bromo-3-chloropropane
BSA	Bovine serum albumin
BCA	Bicinchoninic acid
Dcytb	Duodenal cytochrome b
DFO	Desferrioxamine mesylate
DMEM-F12	Dulbecco's modified eagle medium nutrient mix F12
DMF	Dimethylformamide
DMSO	Dimethyl sulphoxide
DMT1	Divalent metal transporter 1
DTPA	Diethylenetriaminepentaacetic acid
DTT	Dithiothreitol
EDTA	Ethylene diamine tetraacetic acid
FBS	Fetal bovine serum
Fpn	Ferroportin
GFP	Green Fluorescent protein
HBSS	Hanks balanced salt solution
HCP1	Heme carrier protein 1
HEPES	N, 2-Hydroxyethylpiperazine-N'-2-ethane sulfonic acid
HFE	Human gene for HH
HJV	Haemojuvelin
IPTG	Isopropyl ß-D-1 thiogalactopyranoside
IRE	Iron response element
IREG1	Iron regulated transporter 1
IRP	Iron response protein
ITS	Insulin-Transferrin-Selenium Supplement
LCI	Long coding isoform
LUI	Long untranslated isoform
MOPS	4-morpholinepropanesulfonic acid
MT-1	Metallothionein

MTF-1	Metal response element-binding transcription factor
NTBI	Non-transferrin-bound iron
PBS	Phosphate buffered saline
PCR	Polymerase chain reaction
SDS	Sodium dodecyl sulphate
SDS-PAGE	Sodium dodecyl sulphate-polyacrylamide gel electrophoresis
SCI	Short coding isoform
STEAP3	Six-transmembrane epithelial antigen of prostate protein 3
SUI	Short untranslated isoform
TBI	Transferrin-bound iron
Tf	Transferrin
TfR1	Transferrin receptor 1
TfR2	Transferrin receptor 2
UTR	Untranslated region
X-gal	5-bromo-4-chloro-3-indoyl-ß-D- Galactoside N, N-dimmethylformamide
ZIP14	Zinc-regulated transporter and iron-regulated transporter-like protein 14
ZnT-1	Zinc transporter 1 gene

ABSTRACT

Hereditary haemochromatosis is an autosomal recessive disorder of iron metabolism, characterised by increased iron absorption and progressive iron accumulation particularly in the liver. It has been shown that hepatocytes can acquire iron in two forms; transferrin-bound iron (TBI) and non-transferrin-bound iron (NTBI)[1]. Known transporters of NTBI into the cell include DMT1 and ZIP14, and FPN is the only transporter known to export iron.

The aims of this study were to characterize the zinc transporter, *ZnT-1* and determine whether it is involved in iron transport, specifically as an exporter.

There was a decrease in mRNA expression of the short untranslated isoform of *ZnT-1* in double mutant (Hfe -/- and TfR2 Y245X) mouse liver, a trend also seen in *TfR1* and *Hamp*. The long untranslated isoform, however, was significantly higher in the iron-deficient mice as was expression of *TfR1* and *Ferroportin*. Iron and zinc efflux was measured in cells over-expressing *ZnT-1* and control cells. There was no difference between over-expressed and control cells in iron efflux. However, at 60 min, over-expressed cells had significantly more zinc efflux than control cells. More zinc than iron was released from the cell.

The results of this study do not support the hypotheses that (i) *ZnT-1* reduces intracellular cytoplasmic iron concentration by promoting efflux and [2] *ZnT-1* is down-regulated in iron-loaded cells.

Chapter 1

Introduction

1.1 The Importance of Iron

Iron is vital for most living organisms as it is essential for numerous metabolic processes including oxygen transport, DNA synthesis, energy production and electron transfer[3]. Additionally it is a co-factor in proteins including those involved in crucial enzymatic processes[4]. Iron has the capacity to cycle between ferric (Fe^{3+}) and ferrous (Fe^{2+}) forms through the donation or acceptance of an electron[5]:

$$\mathbf{Fe^{3+} + O_2^{-} \longrightarrow Fe^{2+} + O_2}$$

This capability makes iron highly important in biological systems[6]. However, under physiological conditions, ferrous iron is almost insoluble and potentially toxic due to the generation of highly reactive free radicals such as O_2 and OH^-, resulting in tissue damage[5]. Therefore, iron's availability must be regulated carefully to maintain homeostasis and prevent iron disorders such as iron deficiency and iron overload[4].

1.2 Iron disorders

Since the human body has not evolved a mechanism to clear excess iron, disorders of iron balance, such as iron overload and iron deficiency, are common diseases in humans[7].

Iron deficiency is the most common known form of nutritional deficiency. Its causes include inadequate intake, blood loss and interference with absorption due to substances in the diet or drugs[8]. Conversely, iron overload disorders are diseases caused by the accumulation of iron in the body. Primary iron overload is generally due to a genetic factor resulting in a disease such as haemochromatosis,

and secondary iron overload is an acquired condition due to excessive absorption of dietary iron, repeated blood transfusions and other chronic liver disease such as cirrhosis and hepatitis C[9]. However, given the focus of this study, discussion will be limited to haemochromatosis.

1.2.1 Haemochromatosis

Hereditary haemochromatosis (HH) is a disease that causes the body to absorb too much iron from the diet leading to the accumulation of iron in organs including the liver, heart, pancreas and gonads[5]. Body iron stores accumulate slowly with the majority of patients presenting with symptoms at the age of 40 – 60 years[4]. The most common, HH type 1 is transmitted in an autosomal recessive fashion and represents more than 90% of iron-overload syndromes of genetic origin[10]. Furthermore, it is the most common genetic disorder among Caucasians of northern European descent, with a prevalence of 1:190 in Australia[11]. HH type 1 occurs as a result of a mutation in the *HFE* gene. First identified in humans in 1996, the *HFE* gene is located on the short arm of chromosome 6. HFE is a 343 amino acid protein with homology to the major histocompatibility complex (MHC) class I molecules. In HH type 1, a C282Y mutation to the *HFE* gene causes altered folding of the protein preventing its transport to the cell surface, thereby disabling its ability to down-regulate cellular iron uptake[12]. The less common H63D mutation is not associated with the same degree of iron overload as the C282Y mutation[13].

Juvenile or HH type 2 is a rare autosomal recessive disorder which causes progressive elevated iron absorption with clinical symptoms appearing usually at

the age of 20 – 30 years. There are two genetic forms of HH type 2; type 2A, the most common form is caused by mutations in the *hemojuvelin* gene (*HJV*) and type 2B is caused by mutations in the *hepcidin* gene (*HAMP*)[9].

HH type 3 is a rare autosomal recessive disorder resulting in elevated iron absorption due to mutations in the *transferrin receptor 2* gene (*TfR2*). First described in four families as a homozygous nonsense mutation (Y250X)[14], several mutations have since been characterised. HH type 3 is a more severe form of HH and clinical and pathological characteristics resemble those of classic HFE-related HH[15].

HH type 4, also known as ferroportin disease type B[16] or ferroportin-associated iron overload[17], is an autosomal dominant disorder which causes elevated iron absorption due to a mutation involving three sequential bases in exon five[17] in the *ferroportin 1* gene (*FPN1*). Although there is a severe iron load, the phenotype appears to be mild and liver disease is limited to fibrosis, primarily sinusoidal[17].

1.2.2 *Hfe* Gene Knockout (KO) Mouse Model of HH Type 1

The *Hfe* KO mouse model was created in 1998 by Zhou *et al*. by homologous recombination resulting in a disrupted *Hfe* gene. The *Hfe* KO mice are homozygous for the null allele and exhibit abnormally high transferrin saturation and excessive accumulation of iron in the liver, predominantly in the hepatocytes[18].

1.2.3 *TfR2* Mutant Mouse Model of HH Type 3

The *TfR2* mouse model was developed in 2002 by introducing a premature stop codon (Y245X) in the *TfR2* coding sequence by targeted mutagenesis. Orthologous to the Y250X mutation identified in patients with HH type 3, the homozygous *TfR2* (Y245X) mutant mice show profound abnormalities in iron homeostasis and demonstrate elevated transferrin saturations[19].

1.2.4 *Hfe -/-/TfR2* Y245X Double Mutant Mouse Model

The *Hfe -/-/TfR2* Y245X mouse model was recently developed by breeding *Hfe* and *TfR2* mice to homogeneity on a AKR background to generate mutants homozygous for each gene disruption. The double mutants have more severe loading compared to mice carrying the *Hfe* or *TfR2* mutation alone resulting in a more severe early onset with a phenotype similar to HH type 2[20; 21; 22].

1.3 Distribution of Iron in the Body

Body iron stores are approximately 45 to 55 mg per kilogram of body weight in an adult male and approximately 35 to 45 mg per kilogram of body weight in a premenopausal woman[6]. However, after menopause and the cessation of menstruation, iron stores increase[23]. Body iron stores are maintained at a steady state because dietary iron intake is balanced by normal, gradual iron loss[4].

Iron homeostasis is primarily maintained by regulating the absorption of iron from the diet as well as its distribution within the body[24]. Dietary iron is absorbed in the duodenum by enterocytes and circulates in the plasma bound to transferrin and is

utilised by tissues throughout the body. Circulating red blood cells comprise the largest iron storage pool, and when senescent red blood cells are engulfed by reticuloendothelial macrophages, iron is made available for redistribution to other tissues such as the liver which is the main site of iron storage. Most of the circulating iron is used by the bone marrow to generate haemoglobin for red blood cells, while around 10 – 15% is used by muscle fibres to generate myoglobin. About 1 – 2 mg of iron is lost each day via, cell shedding from the skin, sloughed mucosal cells, menstruation or other blood loss (Figure 1.1)[6].

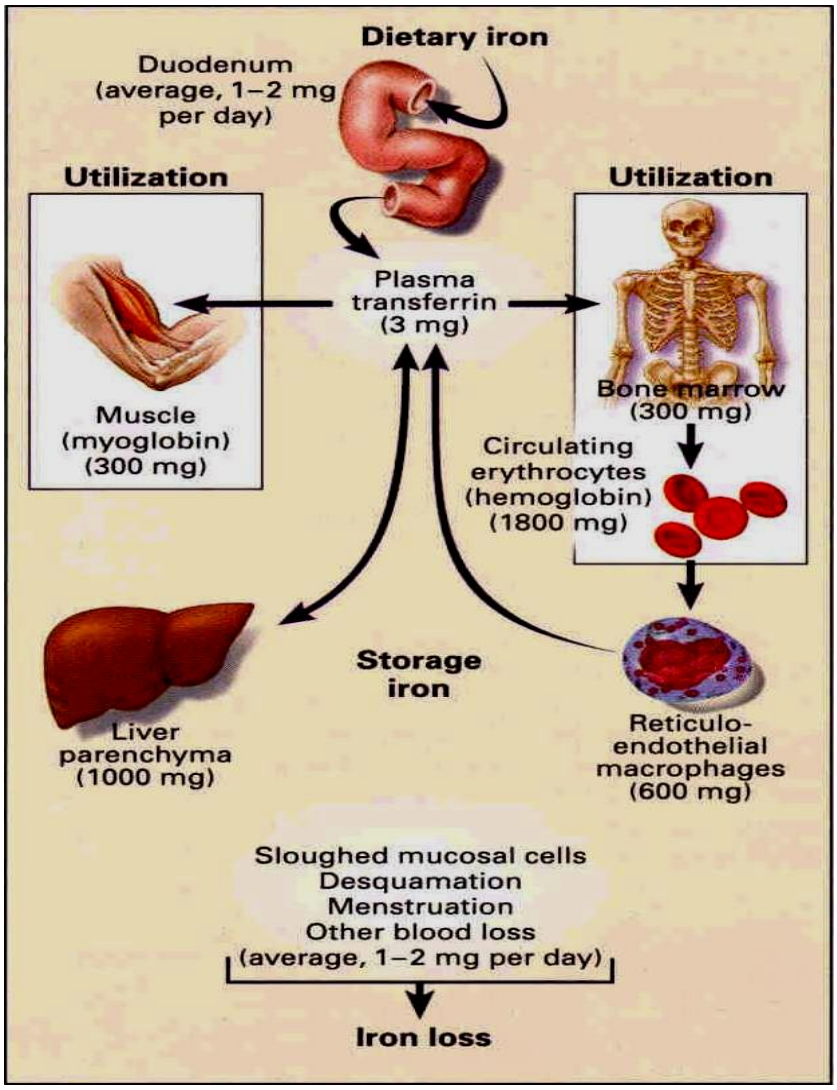

Figure 1.1: Distribution and content of iron in the adult body. Reproduced from Andrews[6].

1.4 Intestinal Iron Absorption

Dietary iron absorption takes place in the duodenum across the apical membrane of mature enterocytes. Haem iron is transported into the cell by a carrier yet to be identified[25]. Non-haem iron is imported into the cell by the divalent metal transporter protein (DMT1)[26]. After enzymatic reduction from Fe^{3+} to Fe^{2+} by duodenal cytochrome *b* (Dcytb), and uptake by DMT1, non-haem iron can either be stored within the cell as ferritin, or transferred across the basolateral membrane into the blood by ferroportin, also known as iron regulated transporter 1 (IREG1)[25]. Iron release is facilitated by hephaestin which assists ferroportin by oxidizing iron for loading on to transferrin in the plasma[27] (Figure 1.2). Iron absorption is also regulated by hepcidin, the hepatic iron regulatory hormone which binds to ferroportin molecules on the surface of duodenal enterocytes and mediates its degradation, thus inhibiting the export of iron from the enterocytes[16].

Haem iron absorption is thought to be mediated by a carrier which is yet to be identified[25]. Upon entering the cell, haem iron is degraded by haem oxygenase and the released ferrous iron appears to join the same intracellular pathway as non-haem iron[26] (Figure 1.2).

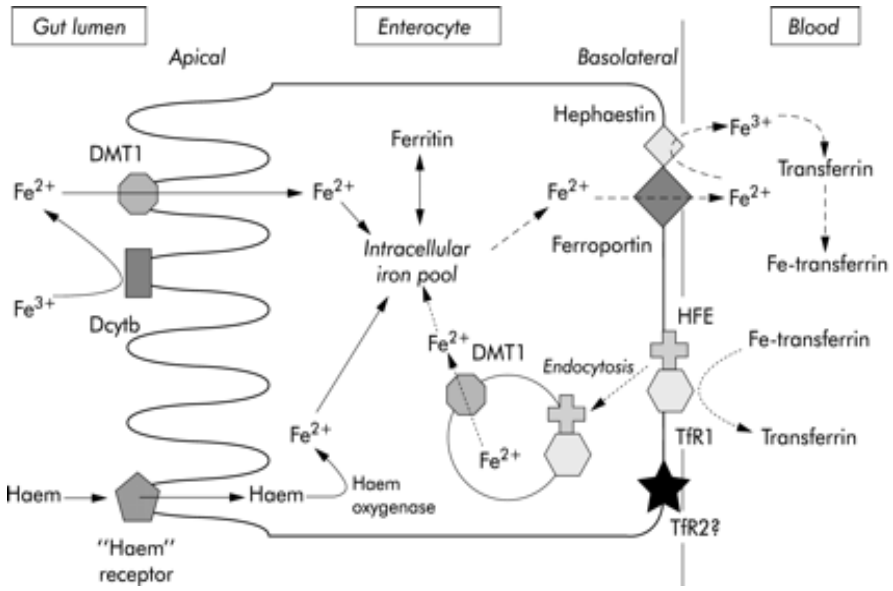

Figure 1.2: Absorption of iron in the gut. Iron absorption occurs across the apical membrane into enterocytes and is either stored in ferritin or transferred across the basolateral membrane into the blood. Reproduced from Trinder *et al.*[28].

1.5 Cellular Iron Uptake and Storage

The majority of iron is transported in the plasma bound to transferrin which maintains iron in a soluble form at near neutral pH and prevents free radical formation[3]. Each transferrin molecule binds two atoms of ferric iron[29] and allows it to be transported between the sites of absorption, storage and use by body organs[3]. Transferrin-bound iron (TBI) is mediated by cell surface receptors transferrin receptor 1 (TFR1) and transferrin receptor 2 (TFR2)[30].

Iron also circulates in a chelatable, low molecular weight form and the main species is ferric citrate. Known transporters of non-transferrin-bound iron (NTBI) include DMT1 and zinc-regulated transporter and iron-regulated transporter-like

protein 14 (ZIP14)[31], which first discovered to transport zinc, has recently been reported to transport iron in an *in vitro* model[32].

1.6 Hepatic Iron Transport

The liver is the main site of iron storage and iron is stored as ferritin or haemosiderin[29]. Figure 1.3 shows how under conditions of normal iron homeostasis, transferrin-bound iron binds to TFR1 or TFR2 and is taken up by receptor-mediated endocytosis. The endosome is acidified and Fe^{3+} is reduced by six-transmembrane epithelial antigen of prostate protein 3 (STEAP3). The iron is released and transported out of the endosome via DMT1 and apotransferrin (iron-free) is exocytosed. Uptake of NTBI occurs via reduction on the hepatocyte surface by a ferrireductase and transported by DMT1 or ZIP14. Iron within the transit pool is stored as ferritin or released from the cell by ferroportin (FPN) where it is oxidized by caeruloplasmin and binds to apotransferrin.

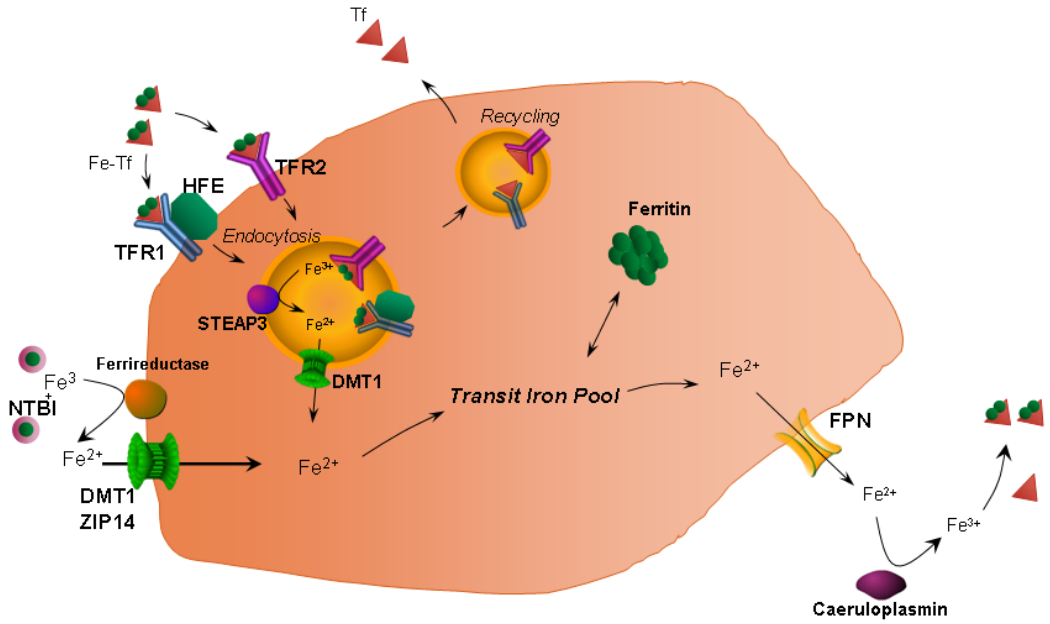

Figure 1.3: Iron Transport in the Hepatocyte. Iron is transported into the cell as TBI or NTBI where it is stored as ferritin. Iron is released by FPN where it binds to apotransferrin. Adapted from Graham *et al.*[31].

The cellular uptake of transferrin bound iron is controlled by regulating the expression of TFR1 through iron response elements (IRE) that regulate the transcription of transferrin receptors[33]. IREs are located in the untranslated region of mRNAs and are responsive to iron[34]. When iron levels are low, iron response proteins (IRP) bind to IREs in the 3' untranslated region of *TFR1* mRNA which stabilizes the mRNA and prevents degradation thus increasing its translation[35]. Conversely, when iron levels are high, binding of IRPs to the IRE is decreased and *TfR1* is destabilized resulting in subsequent decreases in protein synthesis and iron transport[36].

Release of iron from the cell is regulated by the liver-produced hormone hepcidin. High iron concentrations lead to the secretion of hepcidin which binds to ferroportin and induces its internalisation and degradation thus preventing iron efflux[37].

While it has been established that TBI is released from the cell via FPN, the mechanism for NTBI export is yet to be explained. It is now known that DMT1 and ZIP14 are capable of transporting more than one metal[31], therefore it is reasonable to suggest a zinc transporter as a possible candidate for the export of iron. Zinc Transporter 1 (ZNT-1) is located on the plasma membrane and transports zinc out of the cell in the same way that ferroportin transports iron so, could ZnT-1 be involved in iron homeostasis?

1.7 Introduction to Zinc

Zinc is a metallic trace element that is essential for human health and development. The adult human body contains about 2 to 3 grams of zinc[38] which is distributed in all body tissues, with 85% of the whole body zinc in muscle and bone, 11% in the skin and the liver and the remaining in all the other tissues[39]. Zinc has been known to be an essential trace element for more than a century; however, it was not until 1940 when Keilin and Mann discovered zinc in carbonic anhydrase that a specific biological role was established[40]. It is estimated that at least 10% of the hundreds of thousands of proteins in the human body contain zinc prosthetic groups[41] and over three hundred of these proteins are involved in crucial enzymatic processes including representatives from all six major functional enzyme classes[42]. In addition, zinc ions have now been recognized as important signalling molecules which activate intracellular pathways via an extracellular zinc sensing receptor (ZnR)[43]. These pathways regulate key cell functions such as cell proliferation and survival[44], ion transport[45] as well as hormone secretion[43]. Consequently, mechanisms exist to ensure that adequate intracellular zinc concentrations are maintained in order to support these essential roles regardless of whether extracellular or dietary levels are minimal or excessive[46].

1.8 Zinc Homeostasis

Homeostasis is maintained through a regulated rate of intestinal uptake, faecal and to a lesser extent urinary excretion, renal reabsorption and distribution to cells[47]. Zinc is absorbed by the small intestine[48] and released into the portal circulation where, after binding with albumin and α2-macroglobulin[49], it is taken up across

the plasma membrane into the cytosol where only a small amount, well below nanomolar levels, of free zinc remain[47]. The balance is thought to be available for three additional intracellular pools (Figure 1.4)[47]. Zinc binds tightly to metalloproteins as a structural component or a cofactor[42]. In addition, low affinity metallothioneins bind zinc; this is believed to provide an important labile pool thought to be a reservoir and buffer of cytosolic zinc[50]. Furthermore, zinc is compartmentalized into intracellular organelles such as mitochondria, the endoplasmic reticulum (ER), and the Golgi apparatus, as well as specialized organelles such as synaptic vesicles and secretory granules to be used by zinc-dependent proteins[47]. In addition, zinc is transported into an endosomal/lysosomal compartment thought to be facilitated by ZnT-2[51]. Gaither and Eide hypothesised the binding of zinc to metallothionein proteins along with sequestration within organelles or efflux across the plasma membrane to serve as a detoxification mechanism[46].

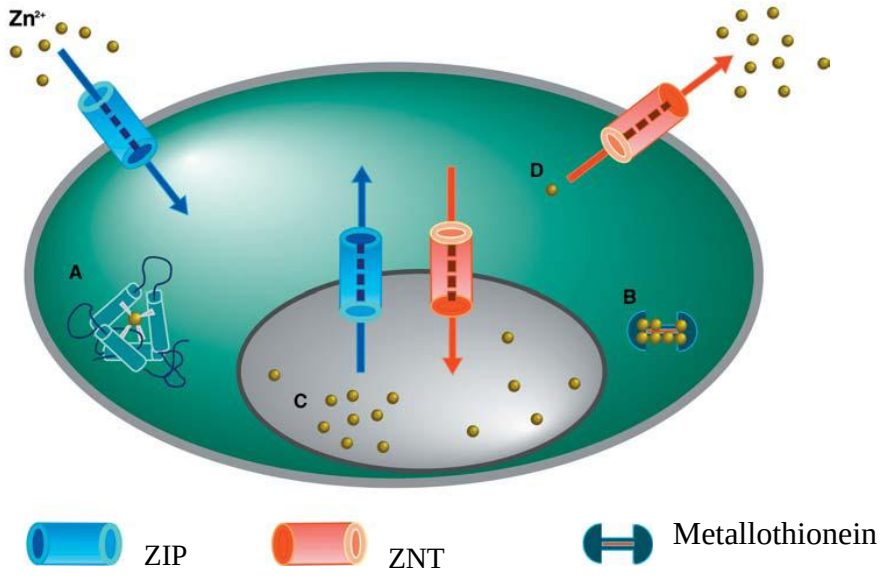

Figure 1.4: Zinc Transporters. The transport of zinc into or out of cytoplasm is directed by two zinc transporter families, the ZIP family are involved in the uptake of zinc and ZnT family are involved in zinc efflux. Zinc in mammalian cells exists in four distinct pools; (*A*) Zinc in cytoplasm is tightly bound to metalloproteins as a structural component or as a cofactor or (*B*) loosely bound to metalloproteins to reserve zinc. (*C*) Zinc is compartmentalized in intracellular organelles. (*D*) The free zinc concentration in the cytosol is estimated to be well below a nanomolar level. Reproduced from Kambe *et al*.[47].

1.9 Zinc Transporters

Central to the movement of zinc into or out of the cytoplasm are the zinc transport proteins. To date, known mammalian zinc transporters come mainly from two families, ZnT/CDF and ZIP[52], both of which are part of the solute carrier (SLC) group of transport proteins and, hence, are also referred to as SLC30 and SLC39, respectively[53]. By convention, members within an individual SLC family have greater than 20% sequence homology to each other; however, the homology between SLC families is very low to non-existent[53]. Therefore, the criteria for inclusion of a family into the SLC group are functional[53]. ZnTs and ZIPs appear to have opposing roles; ZnTs reduce intracellular cytoplasmic zinc by promoting zinc efflux or compartmentalization, while ZIPs are involved in the uptake of zinc

from outside the cell into the cytoplasm as well as transporting it from intracellular organelles into the cytoplasm[52] (Figure 1.4). Since this project involves the characterization of ZnT-1, discussion will be limited to this transporter.

1.9.1 Zinc Transporter 1

ZnT-1 was the first zinc transporter to be discovered, it was mapped to chromosome one in humans and, with two exons, it has the simplest structure of the ZnT family[54]. cDNA predicts a 507 amino acid protein with six predicted transmembrane domains[46] and cytoplasmic amino and carboxy termini[55]. In addition, the ZnT proteins have histidine rich motifs usually in the cytoplasmic loop between transmembrane domain IV and V, which is thought to act as a metal binding domain[56] (Figure 1.5). Furthermore, alterations within this loop affect its metal specificity, suggesting it is also involved in metal recognition[47].

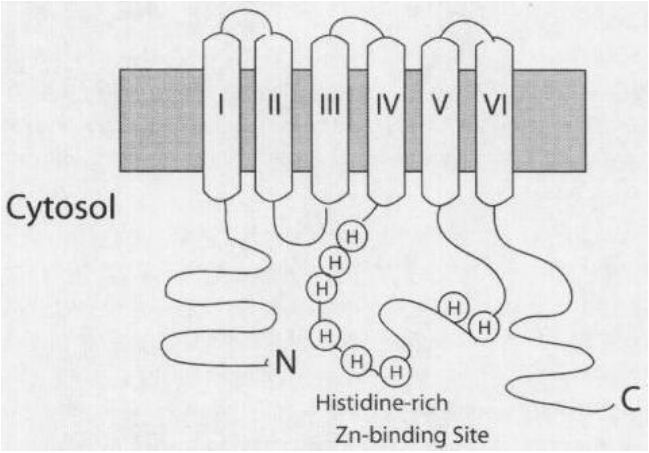

Figure 1.5: Typical structure of a ZnT zinc transporter. A six transmembrane domain integral protein with cytosolic C and N termini, as well a histidine-rich loop. Reproduced from Harris[56].

Palmiter and Findley reported zinc efflux and a reduced concentration of intracellular zinc in cells over-expressing *ZnT-1*, furthermore imunocytochemistry revealed localisation to the plasma membrane suggesting that ZnT-1 was involved in transporting zinc out of the cell[57]. To date it is the only member of the SLC30 family whose prime location is on the plasma membrane[58].

Although *ZnT-1* mRNA is ubiquitously expressed, its abundance differs among tissues[59], however it is particularly abundant in intestine, liver[60], kidney, placenta[47] and the brain[61]. McMahon and Cousins, reported two transcript sizes for *ZnT-1* mRNA and suggest that this is a result of mRNA processing[60]. Expression is regulated by dietary zinc[60] which is believed to occur by a mechanism involving the metal response element-binding transcription factor (MTF)-1 which binds actively to two metal-response element sequences on the *ZnT-1* promoter[62]. Protein expression has been reported to be highly expressed in the brain[61], epithelium of the esophageus, duodenum of the small intestine, caecum of the large intestine[63], and the liver[60]. However, Western blot analysis of intestine and liver tissues detects two different sized proteins suggesting that the protein is subject to post-translational modifications in a tissue-dependent manner[47].

1.10 Microarray Analysis of ZnT-1

Recently, Microarray analysis was performed to determine *ZnT-1* expression in liver from wild type, iron-loaded and TfR2 Y245X mutant mouse models[64]. Probes targeted two areas of the *ZnT-1* mRNA, designated short untranslated isoform (SUI) and long untranslated isoform (LUI), for the 5' untranslated region

and 3' untranslated region of the mRNA respectively. The results showed a decreased level of expression of the *ZnT-1* SUI in iron-loaded and TfR2 Y245X mice compared to wild type mice (Figure 1.6).

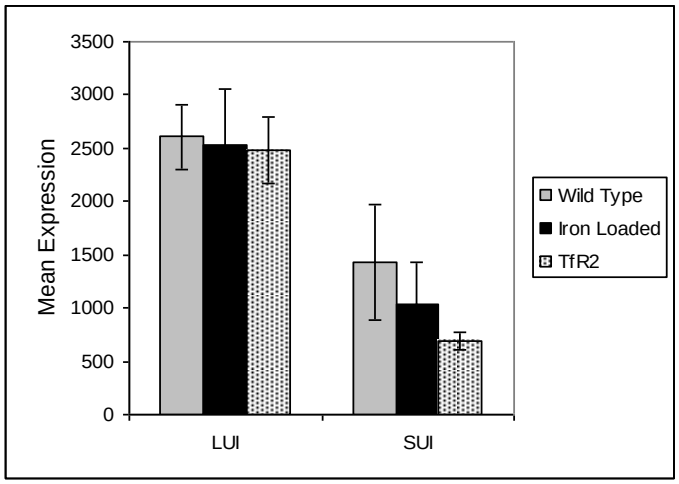

Figure 1.6: Microarray of *ZnT-1* LUI and SUI. Results are expressed as mean ± SD. There was a decreased level of expression of the *ZnT-1* SUI in iron-loaded and TfR2 Y245X mice compared to wild type mice.

1.11 Statement of Aims

ZNT-1 is located on the plasma membrane and is involved in zinc efflux. It has now been established that DMT1 and ZIP14 are capable of transporting more than one metal, therefore it is reasonable to suggest a zinc transporter as a possible candidate for the export of iron. This project aims to determine whether ZnT-1 is involved in iron transport.

1.12 Hypotheses

1) ZnT-1 reduces intracellular cytoplasmic iron concentration by promoting efflux.

2) *ZnT-1* is down regulated in iron-loaded cells and contributes to hepatic iron loading characteristic of haemochromatosis.

1.13 Research Plan

Aim 1: To analyse liver *ZnT-1* expression in wild-type mice fed either a control, iron-deficient or iron-loaded diet, Hfe knockout, TfR2 mutant and Hfe x TfR2 double mutant mouse models of HH and in hepatic cells over-expressing the *ZnT-1* gene.

RNA was extracted from mouse liver and reverse transcribed to generate cDNA to be used in RT-PCR analysis. RT-PCR was used to amplify a region of the gene that quantifies the level of *ZnT-1* transcript as well as *Fpn*, *TfR1* and *Hamp*. In addition, RNA was extracted and mRNA expression of *ZnT-1*, *Fpn*, *Dmt1* and *Zip14* was analysed by RT-PCR.

Aim 2: To clone *ZnT-1* into a Gateway® vector with a Green Fluorescent Protein (GFP) N-terminal tag.

The *ZnT-1* coding sequence of the gene was amplified by PCR using primers designed with *att*B sites to facilitate cloning into a Gateway® vector to produce an entry clone which was subjected to a number of screening processes including, PCR, agarose gel electrophoresis and sequencing before being cloned into a Gateway® destination vector to generate an expression clone.

Aim 3: To determine the cellular localisation of ZnT-1

AML12 mouse hepatocytes were transfected with the expression clone to produce a GFP ZnT-1 fusion protein which was visualised by fluorescence microscopy to determine its cellular location. In addition protein was extracted from the cells and Western immunoblotting was performed to confirm protein expression.

Aim 4: To measure iron and zinc uptake and release in cells over expressing *ZnT-1*.

AML12 cells over expressing ZnT-1 and non-transfected cells were loaded with radio-labelled zinc and iron and the amount of zinc and iron taken up and released by the cells was measured.

Chapter 2

Materials and Methods

2.1 MATERIALS AND EQUIPMENT

2.1.1 RNA Extraction, DNase Treatment and Quantification

Item	Supplier
Biological Safety Cabinet (Gelman BH-2000 Cabinet Class II)	Gelman Sciences, Australia
Block Heater (Thermolyne)	Laboratory Supply, Australia
BCP Phase Separation Reagent (1-Bromo-3-chloropropane)	Sigma-Aldrich, USA
rDNase 1 (2U/µL)	Ambion Inc, USA
DNase 1 Buffer (10x)	Ambion Inc, USA
DNase Inactivation Reagent	Ambion Inc, USA
Absolute Ethanol (C_2H_5OH)	BDH Merck Pty Ltd, Australia
Homogeniser (Ultra-Turrax T25)	John Morris Scientific, Australia
Isopropanol (C_3H_8O)	BDH Merck Pty. Ltd., Australia
Spectrophotometer (DU 640)	Beckman Coulter, USA
Tri-Reagent (RNA Isolation Reagent)	Ambion Inc, USA

2.1.2 Reverse Transcription, RT-PCR and PCR

Item	Supplier
Dimethyl Sulphoxide (DMSO)	Sigma-Aldrich, USA
Dithiothreitol (DTT) 0.1 M	Invitrogen, Australia
DNA Polymerase: HiFi Platinum *Taq*, *Pfx*50, *Pfu* and Platinum *Taq* (5 U/µL)	Invitrogen, Australia
dNTPs (100 mM)	Fisher Biotec, Australia
Ethylenediaminetetraaceticacid (EDTA)	Merck, Germany

First Strand RT Buffer (5x)	Invitrogen, Australia
Magnesium Chloride ($MgCl_2$) (50 mM)	Invitrogen, Australia
Magnesium Sulphate ($MgSO_4$) (50 mM)	Invitrogen, Australia
Oligo dT Primer (0.5 mg/mL)	Promega Corp, USA
PCR Buffer: HiFi Platinum *Taq*, *Pfx*50, *Pfu* and Platinum *Taq* (10x)	Invitrogen, Australia
PCR Enhancer Solution (10x)	Invitrogen, Australia
PCR Enhancer, Q Solution (5x)	QIAGEN, Australia
Primers	Invitrogen, Australia
Real-Time Cycler (Corbett Research RG 2000 & 3000)	Fisher Biotec, Australia
Reverse Transcriptase, Superscript III (200 U/µL)	Invitrogen, Australia
RNasin RNase Inhibitor (40 U/µL)	Promega Corp, USA
SYBR Green (10x)	Invitrogen, Australia
Thermal Controller (PTC-100TM)	Gene Works Pty Ltd, Australia
Tris	BDH AnalaR, Australia

2.1.3 Agarose Gel Electrophoresis

Item	**Supplier**
Agarose (Analytical Grade)	Promega Corp, USA
Ethylenediaminetetraaceticacid (EDTA)	Merck, Germany
Ethidium Bromide (10 mg/mL)	Promega Corp, USA
Gel Tank	Bio-Rad Laboratories, USA/Fisher Biotec, Australia
Glacial Acetic Acid (CH_3COOH)	Merck, Germany
6x Loading Dye (Blue/Orange)	Promega Corp, USA

1 Kb Plus Molecular Weight Marker	GIBCO™ Invitrogen, Australia
Power Pac 300	Bio-Rad laboratories, USA
Tris	BDH AnalaR, Australia
VersaDoc Imaging System 3000	Bio-Rad Laboratories, USA

2.1.4 Cloning

Item	**Supplier**
Ampicillin	Sigma-Aldrich, USA
Bacto Agar	Bacto Laboratories, Australia
Bacto Tryptone	BD Beckton, Dickinson & Co, USA
5-bromo-4-chloro-3-indoyl-ß-D- Galactoside N, N-dimmethylformamide (X-gal)	Fisher Biotec, Australia
Centrifuge (Beckman J2-MI and JA17 rotor)	Beckman Instruments, Australia
ChargeSwitch®-Pro PCR Clean-up Kit	Invitrogen, Australia
Cryotubes (2 mL)	Sarstedt AG & Co, USA
Disposable Inoculating Loops (1 µL)	Copan, Italy
Dimethylformamide (DMF)	Sigma-Aldrich, USA
E. coli DH5-α	Invitrogen, Australia
FastPlasmid™ Mini Kit	Eppendorf, Australia
Gateway® Technology PCR Cloning System	Invitrogen, Australia
Glucose	Sigma, USA
Incubator Shaker (Innova 4000)	John Morris Scientific, Australia
Isopropyl ß-D-1 thiogalactopyranoside (IPTG)	Sigma-Aldrich, USA
Kanamycin	Sigma-Aldrich, USA
Potassium chloride (KCl)	BDH AnalaR, Australia

Magnesium chloride hexahydrate ($MgCl_2.6H_2O$)	BDH AnalaR, Australia
Magnesium sulphate heptahydrate ($MgSO_4.7H_2O$)	BDH GPR™, UK
Sodium chloride (NaCl)	Merck, Germany
Petri Dish (90 x 14 Full Plate)	Sarstedt, Australia
pGEM®-T Easy Vector System	Promega Corp, USA
PureLink™ PCR Purification Kit	Invitrogen, Australia
PureLink™ HiPure Plasmid Filter Purification Kit	Invitrogen, Australia
QIAquick® Gel Extraction Kit	QIAGEN, Australia
QIAGEN Plasmid Maxi Kit	QIAGEN, Australia
QIAprep® Spin Miniprep Kit	QIAGEN, Australia
Spectrophotometer (DU 640)	Beckman Coulter, USA
Yeast Extract	Oxoid, Australia

2.1.5 Cell Culture & Fluorescence Microscopy

Item	**Supplier**
Acetone ($(CH_3)_2CO$)	Sigma-Aldrich, USA
Biological Safety Cabinet (Gelman BH-2000 Cabinet Class II)	Gelman Sciences, Australia
Culture Plates (MULTIWELL™ 6-Well)	BD Falcon, USA
Culture Plates (MULTIWELL™ 12-Well)	BD Falcon, USA
Culture Slide (4 Chamber Tissue Culture treated Glass Slide)	BD Falcon, USA
Dexamethasone	Sigma, USA
Dulbecco's modified eagle medium nutrient mix (DMEM-F12)	GIBCO™ Invitrogen, Australia

Foetal Bovine Serum (FBS)	GIBCO™ Invitrogen, Australia
Gentamicin (40 mg/mL)	Pfizer, Australia
Haemocytometer (Brand)	Hirschmann EM Techcolor
Immersion Oil	Nikon, Japan
Incubator (CO_2 Forma Series II Water Jacketed HEPA Class 100)	Forma Scientific Inc, USA
Insulin-Transferrin-Selenium (ITS) Supplement Premix (100x)	BD Biosciences, USA
L-glutamine	GIBCO™ Invitrogen, Australia
Methanol (CH_3OH)	BDH Laboratory Supplies, UK
Sodium bicarbonate ($NaHCO_3$)	BDH AnalaR, Australia
Microscope (Eclipse TE2000-U with DS Camera DS-L1)	Nikon, Japan
Microscope (Olympus CK2)	Olympus, Japan
Needle (23 G Precision Glide)	Becton Dickson, Singapore
Phosphate Buffered Saline powder (PBS)	Thermo Electron, Australia
Prolong® Gold antifade reagent with DAPI	Invitrogen, Australia
Syringe (1 mL)	Terumo Corporation, Philippines
Tissue Culture Flask (Nuclon™ΔSurface 75 cm^2 Vented)	Nunc™, Denmark
Trypsin-EDTA	Sigma-Aldrich, USA

2.1.6 Transfection

Item	**Supplier**
Biological Safety Cabinet (Gelman BH-2000 Cabinet Class II)	Gelman Sciences, Australia
Lipofectamine™ LTX Reagent	Invitrogen, Australia
Opti-MEM® I Reduced Serum Medium	GIBCO™ Invitrogen, Australia

PLUS™ Reagent (3 mg/mL)	Invitrogen, Australia

2.1.7 Protein Extraction and Quantification

Item	**Supplier**
Biological Safety Cabinet (Gelman BH-2000 Cabinet Class II)	Gelman Sciences, Australia
Cell Scraper (25 cm, 2 position blade)	Sarstedt Inc., USA
Hydrochloric acid (HCl) (37%)	BDH AnalaR, Australia
Microplate (96-Well)	Greiner Bio-One, Germany
Microplate Reader (FLUOstar Optima)	BMG Glass Inc, USA
Multipipette (Socorex Acura 855)	Interpath Services, Australia
Sodium hydroxide (NaOH)	Merck, Germany
Protease Inhibitor Tablet	Roche Diagnostics Corp, USA
Protein Assay Kit (Pierce BCA)	Progen Industries Ltd., USA
Sodium Dodecyl Sulphate (SDS)	BDH Laboratory Supplies, UK
Sonicator (Microson Ultrasonic Cell Disruptor)	Misonic Inc., USA
Tris	BDH AnalaR, Australia
Triton X-100	BDH AnalaR, Australia

2.1.8 Western Blotting

Item	**Supplier**
Acetic Acid (CH_3COOH)	BDH Merck, Germany
Bromophenol Blue	Fisons Scientific Equipment, UK
Coomassie Brilliant Blue	Fisons Scientific Equipment, UK
QuickPoint™ Electrophoresis Cell	Novex, USA

Electrophoresis Power Supply (EPS301)	Amersham Pharmacia Biotech, Sweden
Filter Paper (Novablot)	GE Healthcare Life Sciences, Australia
Glycerol	BDH Merck Pty Ltd, Australia
Glycine	ICN Biomedical Inc, USA
Heat Sealer (Impulse HN-300D)	HeatShrink Australia
ß-mercaptoethanol	Sigma-Aldrich, USA
Methanol (CH3OH)	BDH Laboratory Supplies, UK
Shaking platform (Belly Dancer)	Storall Life Science, USA
MOPS SDS Running Buffer NuPage® (20x)	Invitrogen, Australia
Nitrocellulose Blotting Membranes (Bio Trace NT)	Fisher Biotec, Australia
Phosphate Buffered Saline powder (PBS)	Thermo Electron, Australia
Platform Mixer	Ratek Instruments, Australia
Pre-Cast 10 and 12 Well Gels (NuPAGE® 4-12% Bis-Tris Gel)	Invitrogen, Australia
Protein Standard (MagicMark™ XP)	Invitrogen, Australia
Protein Standard (Novex Sharp Pre-stained)	Invitrogen, Australia
Sodium Dodecyl Sulphate (SDS)	BDH Laboratory Supplies, UK
Skim Milk Powder	Woolworths, Australia
Transfer Block (Owl)	Bio-Rad Laboratories, USA
Tris	BDH AnalaR, Australia
NuPAGE® Transfer Buffer	Invitrogen, Australia
VersaDoc Imaging System 3000	Bio-Rad Laboratories, USA
Western Lightning™ *Plus*-ECL (Enhanced Luminol Reagent *Plus*, Oxidising Reagent *Plus*)	Perkin Elmer, USA

Antibodies

β-Actin Goat Polyclonal IgG (200 µg/mL)	Santa Cruz Biotechnology, USA
Donkey Anti-Goat IgG Horseradish Peroxidase Conjugate (200 µg/0.5 mL)	Santa Cruz Biotechnology, USA
Rabbit Polyclonal GFP Antibody (0.5 µg/mL)	Abcam, USA
Goat Anti-Rabbit IgG Horseradish Peroxidase Conjugate (200 µg/0.5 mL)	Santa Cruz Biotechnology, USA

2.1.9 Iron and Zinc Uptake/Release Assays

Item	**Supplier**
Bovine Serum Albumin (BSA)	Thermo Electron, Australia
Counting Test Tubes (Plastic Injector & Blow Moulders)	Techno-Plas, Australia
Desferrioxamine mesylate (DFO)	Sigma, USA
Diethylenetriaminepentaacetic acid (DTPA)	Sigma-Aldrich, USA
Gamma Counter (Wallac Wizard 3" 1480)	Perkin Elmer, Australia
Hyrdochloric acid (HCl) (37 %)	BDH AnalaR, Australia
N, 2-Hydroxyethylpiperazine-N'-2-ethane sulfonic acid (HEPES)	GIBCO™ Invitrogen, Australia
Iron (III) chloride hexahydrate ($FeCl_3$)	Sigma-Aldrich, USA
Iron-59 (Radioisotope)	Perkin Elmer, Australia
Sodium hydroxide (NaOH)	Merck, Germany
Trisodium Citrate	BDH AnalaR, Australia
Triton X-100	BDH AnalaR, Australia
Zinc chloride ($ZnCl_2$)	Sigma-Aldrich, USA
Zinc-65 (Radioisotope)	Perkin Elmer, Australia

2.1.10 General Materials and Equipment

Centrifugation & Vortexing

Item	Supplier
Centrifuge (Capsulefuge Tomy PMC-060)	Quantum Scientific, Australia
Centrifuge (Eppendorf Mini Spin)	Crown Scientific, Australia
Centrifuge (Eppendorf 5424)	Quantum Scientific, Australia
Centrifuge (Megafuge 1.0R)	Heraeus Sepatech, Germany
Centrifuge (Sigma 4K15)	John Morris Scientific, Australia
Vortex (MT 17V)	Chiltern Scientific

Water

Distilled Water, DNAse & RNAse Free, was supplied by GIBCO™ Invitrogen, Australia and Milli-Q (deionised) water was prepared using a Milli-Q Plus Water Purification System (Millipore, Australia).

Sterilization

Glassware was soaked in detergent or bleach and washed with deionised water in a dishwasher before autoclaving (Atherton, Australia).

2.2 BUFFERS, REAGENTS, SOLUTIONS AND MEDIA

Buffers, reagents, solutions and media were prepared by weighing chemicals using an ER-120A or Fx-2000 balance (A & D Mercury, Australia), dissolving in deionized water and, when required autoclaved (120°C; 15 psi; 20 min, Atherton,

Australia). pH was measured using a Corning 220 pH Meter (Crown Scientific, Australia).

2.2.1 Reverse Transcription, RT-PCR and PCR

10 mM dNTPs

A mix containing 10 mM of each dNTP was prepared by adding 100 µL each of 100 mM dATP, dCTP, dGTP, and dTTP to 600 µL nuclease free water and stored at -20°C.

500 mM EDTA

0.186 g EDTA was dissolved in 50 mL Milli-Q H_2O by adjusting the pH to 8.0 and adding additional Milli-Q H_2O to a final volume of 100 mL.

1 Kb Plus Molecular Weight Marker

1 µL of 1 Kb Plus DNA Ladder was added to 2 µL 6x loading dye and nuclease free H_2O to 10 µL and stored at -20°C.

Primers

RT-PCR *ZnT* forward and reverse primers were designed using the web-based computer programme Primer 3[65] in order to amplify the four putative isoforms. qF1/qR1 amplifies a long coding isoform (LCI), qF4/qF1 amplifies LCI as well as the short coding isoform (SCI) which is 269 bases shorter than the LCI, qF2/qR2 amplifies a short untranslated region (SUI) and qF3/qR3 amplifies a long

untranslated region (LUI) (Figure 2.1; Table 2.1). qF1/qR1 and qF4/qR1 RT-PCR primers were designed by Ross Graham from the Iron Metabolism Laboratory, School of Medicine and Pharmacology, Fremantle Hospital Campus, University of Western Australia (Table 2.1). *ZnT-1* PCR primers were designed as described in Section 2.4.6.1 by Ross Graham.

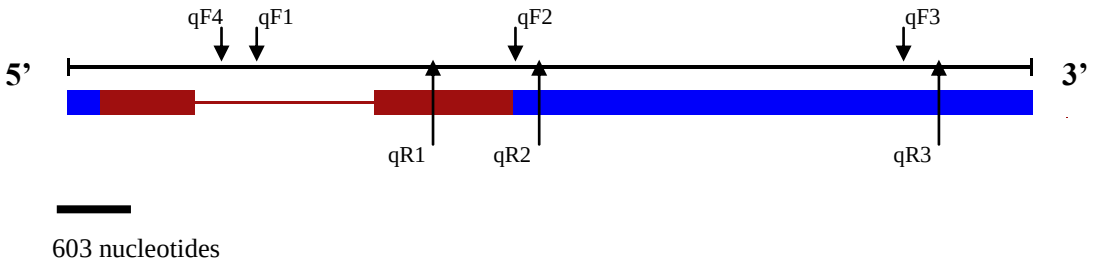

Figure 2.1: *ZnT-1* Primer Sites. Primer sites for the 4 isoforms are shown as well as the coding sequence ■ untranslated region ■ and intron ▬ (adapted from NCBI[66]).

1x SYBR Green

A 1x SYBR Green solution was prepared by adding 100 µL 10x SYBR Green to 900 µL nuclease free water and stored at -20°C.

50x TAE Buffer

121 g Tris was dissolved in 300 mL Milli-Q H_2O before adding 29 mL Glacial Acetic Acid and 50 mL EDTA (500 mM). The volume was made up to 500 mL with Milli-Q H_2O before adjusting the pH to 8.0 and autoclaving.

1x TAE Buffer

200 mL of 50x TAE Buffer was added to 9.8 L Milli-Q H_2O.

1x TE Buffer pH 7.5

1 mL Tris (1 M) and 20 µL EDTA (500 mM) was added to 90 mL Milli-Q H_2O and the pH adjusted to 7.5 before adding additional Milli-Q H_2O to a final volume of 100 mL and autoclaving.

1 M Tris-HCl pH 7.4

12 g of Tris was added to 100 mL Milli-Q H_2O and the pH was adjusted to 7.4.

2.2.2. Cloning

Competent *E. coli* DH5-α Cells

Competent *E. coli* DH5-α Cells were prepared as per Inoue *et al.*[67] by Ross Graham or Carly Herbison from the Iron Metabolism Laboratory, School of Medicine and Pharmacology, Fremantle Hospital Campus, University of Western Australia and storing at -80°C until required.

0.1 M Isopropyl ß-D-1 thiogalactopyranoside (IPTG)

0.2383 g IPTG was dissolved in a final volume of 10 mL Milli-Q H_2O and filter sterilised before being aliquoted into 1.5 mL tubes and storing at -20°C.

2 M Glucose Stock

3.603 g glucose was dissolved in a final volume of 10 mL Milli-Q H_2O and filter sterilised (0.22 µm).

Luria-Bertani (LB) Broth

4 g Bacto Tryptone, 2 g Yeast Extract and 4 g NaCl was diluted in Milli-Q H_2O to a final volume of 400 mL and autoclaved after adjusting the pH to 7.0.

LB Agar

LB Agar was prepared as per LB Broth with the addition of 3 g Bacto Agar.

2 M Mg^{2+} Stock

20.33 g of $MgCl_2.6H_2O$ and 24.65 g $MgSO_4.7H_2O$ was dissolved in a final volume of 100 mL Milli-Q H_2O and filter sterilised (0.22 µm).

SOC

20 g Bacto Tryptone, 5 g Yeast Extract, 5.8 g NaCl and 1.86 g KCl was diluted in 980 mL Milli-Q H_2O and autoclaved after which 10 mL filter sterilised Mg^{2+} (20 mM) was added along with 10 mL filter sterilised glucose (20 mM).

1x TE Buffer pH 8.0

1x TE Buffer was made as outlined in section 2.2.1 with the exception of the pH being adjusted to 8.0.

X-gal (50 mg/mL)

0.2 g of X-gal was dissolved in 10 mL DMF and stored in 1 mL aliquots at -20°C protected from light.

2.2.3 Cell Culture

Dulbecco's Modified Eagle Medium (D-MEM/F12)

One powdered Dulbecco's Modified Eagle Medium (D-MEM/F12) sachet was dissolved in a final volume of 1 L Milli-Q H_2O along with approximately 4 g $NaHCO_3$ to adjust the pH to 7.4 before being filter sterilised and stored at 4°C.

Cell Culture Medium

20 mL Foetal bovine serum (FBS) (10%), 2 mL L-glutamine (2 mM), 0.2 mL Insulin-Transferrin-Selenium Supplement (1x) and 20 µL Dexamethasone (1mM) was added to 180 mL D-MEM/F12 and stored at 4°C. The medium was supplemented with gentamicin (400 µL of 80 µg/mL) .

10x Phosphate Buffered Saline (PBS)

9.55 g Phosphate Buffered Saline powder was dissolved in Milli-Q H_2O to a final volume of 1 L and the pH was adjusted to 7.4 before autoclaving.

1x Phosphate Buffered Saline (PBS)

1x PBS was made by adding 100 mL 10x PBS to 900 mL Milli-Q H_2O, and autoclaving.

2.2.4 Protein Extraction

1 M NaOH

4g of NaOH was dissolved in 100 mL Milli-Q H_2O.

1x Phosphate Buffered Saline (PBS)

1x Phosphate buffered saline was prepared as previously described in section 2.2.3.

10% Sodium Dodecyl Sulphate (SDS)

50 g SDS was added to 500 mL Milli-Q H_2O.

SDS Lysis Buffer (2% SDS, 50mM Tris-HCl pH 7.4)

SDS Lysis Buffer was prepared by adding 2 mL 10% SDS to 500 µL 1 M Tris-HCl pH 7.4 and 7.5 mL Milli-Q H_2O followed by dissolving one protease inhibitor tablet (Chymotrypsin; Pancreas extract; Papain; Pronase; Thermolysin; Trypsin) before storing at -20°C.

Triton/NaOH

1 mL of 1 M NaOH and 100 µL of Triton X-100 were added to 9 mL Milli-Q H_2O.

2.2.5 Western Blotting

Antibodies

ß-Actin Antibodies

5 mL of a 1:1000 concentration of β-Actin Goat Polyclonal IgG (200 µg/mL) primary antibody was prepared in PBST and 5 mL of a 1:2000 concentration of Donkey Anti-Goat IgG Horseradish Peroxidase Conjugate (200 µg/0.5 mL) secondary antibody was prepared in 2% skim milk.

GFP Antibodies

5 mL of a 1:1000 concentration Rabbit Polyclonal GFP (0.5 µg/mL) primary antibody was prepared in PBST and 5 mL of a 1:2000 concentration of Goat Anti-Rabbit IgG Horseradish Peroxidase Conjugate (200 µg/0.5 mL) secondary antibody was prepared in 2% skim milk.

Blocking Solution

5% blocking solution was prepared by dissolving 2.5 g of skim milk powder in 50 mL PBST and storing at 4°C. Similarly a 2% solution was prepared by dissolving 1 g of skim milk powder to 50 mL PBST.

Coomassie Blue Stain Solution

Coomassie Blue Stain solution was prepared by adding 1 g Coomassie Brilliant Blue to 237.5 mL 95% Methanol, 50 mL Acetic Acid and 212.5 mL Milli-Q H_2O.

10x Electrophoresis Buffer (0.025 M Tris pH 8.3, 0.192 M Glycine, 0.1% SDS)

29 g Tris was added to 1 L Milli-Q H_2O along with 144 g glycine and 10 g SDS.

1x Electrophoresis Buffer

A 1x solution was prepared by adding 100 mL 10x Electrophoresis Buffer to 900 mL Milli-Q H_2O.

Loading Dye

25 mg Bromophenol Blue was added to 10 mL 1x Electrophoresis buffer.

1x PBS

1x PBS was prepared as previously described in section 2.2.3.

PBST

1 mL 20% Tween 20 was added to 500 mL 1x PBS.

4x Sample Buffer

4x Sample buffer was prepared by combining 1 mL 2.5 M Tris pH 6.8, 2.7 mL 30% SDS, 4 mL glycerol, 0.3 mL Milli-Q H_2O and 0.5 µL Loading Dye and stored at -20°C. 2 mL 10% ß-Mercaptoethanol was added just prior to use.

30% Sodium Dodecyl Sulphate (SDS)

30 g SDS was added to 100 mL Milli-Q H_2O.

Transfer Buffer (15% Methanol)

10 mL of 20x NuPAGE® Transfer Buffer was added to 160 mL Milli-Q H_2O along with 30 mL of Methanol.

2.5 M Tris, pH 6.8

30 g of Tris was added to 100 mL Milli-Q H_2O and the pH was adjusted to 6.8.

2.2.6 Iron and Zinc Uptake/Release Assays

500 mM Citrate

1.47 g Trisodium citrate was dissolved in 10 mL Milli-Q H_2O.

1 mM $FeCl_3$

2.7 g of $FeCl_3$was dissolved in 10 mL 0.1 M HCl. Then a 1:10 dilution was prepared by adding 10 µL to 9.99 mL of HCl (0.1 M).

HBSS

1 sachet of powdered HBSS was dissolved in 1 L Milli-Q H_2O and approximately 1 g $NaHCO_3$ was added to adjust the pH to 7.4 before being stored at 4°C.

1 M HCl

8.57mL HCl was added to 91.43 mL of Milli-Q H_2O.

0.1 M HCl

1 mL 1 M HCl was added to 9 mL Milli-Q H_2O.

Iron and Zinc Radioactive Solutions

An appropriate dilution of ^{59}Fe and 1 mM $FeCl_3$ or ^{65}Zn and 1 mM $ZnCl_2$ was prepared in 100-fold molar excess of Trisodium citrate and added to 2.8 mL standard uptake/release medium described below. Dilution depended on the specific activity of the radioisotope.

Standard Uptake/Release Medium

DMEM was made as previously described in Section 2.2.3 with 11.92 g HEPES (final concentration, 50 mM), and the pH was adjusted to 7.2. Bovine serum albumin (BSA) was added just prior to use to the required amount of DMEM/HEPES to a final concentration of 2% and incubated at 37°C to dissolve BSA.

Release medium supplemented with DFO

28 µL DFO (10 mM) was added to 2.8 mL standard uptake/release medium to give a final concentration of 100 µM.

Release Medium supplemented with DTPA

11.02 µL DTPA (25.4mM) was added to 2.8 mL standard uptake/release medium to give a final concentration of 100 µM.

Triton/NaOH

Triton/NaOH was prepared as previously described in Section 2.2.4.

1 mM $ZnCl_2$

1.36 g of $ZnCl_2$was dissolved in 10 mL 0.1 M HCl. Then a 1:10 dilution was prepared by adding 10 µL to 9.99 mL of HCl (0.1 M).

2.3 ANIMAL TISSUE AND CELL LINES

Wild type AKR mice were fed a control diet of mouse chow (Specialty Feeds, Glen Forrest, WA) containing 0.01% Fe, an iron-loaded diet containing 2% carbonyl Fe or an iron deficient diet containing 0.001% Fe. *Hfe* knockout, *TfR2*(Y245X) mutant and double mutant (*Hfe* -/-/*TfR* Y245X) mice were fed a control diet. Liver tissue was collected from mice by Ross Graham and Anita Chua (Iron Metablolism Laboratory, School of Medicine and Pharmacology, Fremantle Hospital Campus, University of Western Australia), snap frozen in liquid nitrogen and stored at -80°C until required.

AML12 cells used in this study are a mouse hepatocyte cell line supplied by the American Type Culture Collection, USA. Cells were thawed and subcultured into a 75 cm^2 flask by Carly Herbison.

2.4 METHODS

2.4.1 Extraction of RNA from Liver Tissues

Tissue (40 – 60 mg) was added to a 2 mL microcentrifuge tube containing 400 µL cold TRI Reagent and homogenized using an Ultra-Turrax homogenizer. Then a further 400 µL cold TRI reagent was added to the microcentrifuge tube and incubated at room temperature (RT) for 5 min. After the addition of 80 µL of BCP the tubes were vigorously shaken for 30 s before incubating (10 min, RT). The tubes were centrifuged (16000*g*; 15 min; 4°C) and the aqueous phase containing the RNA was transferred to a 1.5 mL low adhesion microcentrifuge tube. An equal volume of isopropanol was added to pellet the RNA and the tube was mixed by inverting. After incubating for 10 min at RT the tube was centrifuged (16000*g*; 5 min; 4°C) to precipitate the RNA and the supernatant removed. The pellet was washed with 200 µL 75% ethanol, dislodged and centrifuged (8000*g*; 5 min; 4°C). The supernatant was removed and the pellet was air dried before dissolving in 50 µL of nuclease free water (15 min; 55°C).

2.4.2 DNase Treatment of Extracted RNA and Quantification

Following RNA extraction the samples were treated with DNase to remove genomic DNA. A 0.1 volume of 10x DNase 1 buffer and rDNase (2 units) was added to the RNA sample, mixed gently and incubated for 30 min at 37°C). To terminate the reaction, DNase Inactivating Reagent was resuspended and a 0.1 volume was added to the samples and incubated (2 min; RT) with occasional mixing. Centrifugation (10000*g*; 90 s; RT) precipitated the DNase Inactivating Reagent and the supernatant was transferred to a clean 0.6 mL low adhesion

microcentrifuge tube and stored at -80°C until required. The RNA concentration was determined by diluting 2 µL of the sample with 98 µL of nuclease free water (1:50 dilution) and measuring the absorbance at 260 nm and 280 nm by spectrophotometry. Samples with a 260/280 ratio of 1.8 – 2 were considered to be of sufficient purity and used for further analysis where as samples with higher or lower ratios were discarded and RNA was re-extracted from additional samples. RNA concentration (µg/µL) = (A_{260nm} x 40 µg/m x 50)/1000.

2.4.3 Gel Electrophoresis of RNA

RNA integrity was examined by agarose gel electrophoresis. A 1% agarose gel was prepared in 1x TAE buffer and slightly cooled before adding ethidium bromide (0.16 µg/mL). The agarose was poured into a gel tray and allowed to set with the appropriate comb in place. RNA samples were prepared by adding 1.5 µg of RNA up to 10 µL of nuclease free water and heated (70°C; 1 min) before being placed on ice. 5 µL of a 1 Kb Plus molecular weight marker was loaded into the first well. RNA samples were loaded into remaining wells after mixing with 2 µL of 6x loading dye and electrophoresed in 1x TAE buffer (1 h, 120 v). The gel was visualized on a UV transilluminator to verify the presence of the 28S and 18S bands.

2.4.4 Reverse Transcription of RNA

RNA was reverse transcribed to generate complementary DNA (cDNA) in full or half reactions depending on the amount of cDNA required. For a full reaction 2 µg of RNA was diluted in nuclease free water to a final volume of 10 µL. A master mix consisting of Oligo dTs (0.5 µg) and dNTPs (0.5 mM) in nuclease free

water to a final volume of 3.5 µL per RNA sample was prepared and added to each sample before denaturing in a Thermal Cycler (65°C; 5 min) and allowed to cool in a metal cooling block for a minimum of 4 min. 6.5 µL of a master enzyme mix was added to each sample (200U Superscript III reverse transcriptase, 20U RNasin, 5 mM DTT, 1X reverse transcription reaction buffer) and returned to the Thermal Cycler where cDNA was synthesised (50°C; 60 min) followed by an enzyme inactivation cycle (70°C; 15 min). cDNA was stored for a maximum of 3 days at 4°C.

2.4.5 Real-Time Polymerase Chain Reaction (PCR)

Real-time PCR was undertaken on cDNA samples and plasmid standards of known copy numbers (10^1 to 10^{10}) to amplify the gene of interest to quantify mRNA expression. A master mix was prepared for each gene studied and consisted of 0.25 mM dNTPs, 0.25 µM each forward and reverse primer (Table 2.1), 3 mM $MgCl_2$, 0.5 U Platinum *Taq* Polymerase, 0.1x SYBR Green and 1x reaction buffer in nuclease free water to a final volume of 19 µL per sample and aliquoted into tubes to which 1 µL of cDNA or standard was added. The samples underwent PCR in a Corbett Research Real-Time Cycler (RG 2000 or 3000) according to the cycling parameters outlined in Table 2.2.

Table: 2.1 Primers used for real-time RT-PCR of Genes (including Annealing temperature (T_A), Melt Curve Peak and Product Size)

Gene	Primer Sequence (5'- 3')	T_A (°C)	Product Size (bp)
ZnT-1 (LCI)	qF1 CCAACACCAGCAATTCCAAC qR1 AAAAGACCAAGGCATTCACG	59	228
ZnT-1 (SCI)	qF4 GAACGCCATCTTCCTCACG qR1 AAAAGACCAAGGCATTCACG	59	273 (SCI) 542 (LCI)
ZnT-1 (SUI)	qF2 GAGAAGAAGGCCAGGAGGAC qR2 CGACCAGACAAGGACTTCAA	59	210
ZnT-1 (LUI)	qF3 CAGTCATTTTCACTGGCACAA qR3 GACAGGACCAACTCGAGAGC	59	234
ß-actin[68]	F CTGGCACCACACCTTCTA R GGTGGTGAAGCTGTAGCC	59	352
Hamp[69]	F CCTATCTCCATCAACAGATG R AACAGATACCACACTGGGAA	53	171
Fpn[70]	F TTGCAGGAGTCATTGCTGCTA R TGGAGTTCTGCACACCATTGAT	53	120
TfR1[68]	F TTCCTACATCATCTCGCTTAT R CATAGTGTTCATCTCGCCAGA	53	216
Dmt1[71] (Total)	F TCTATCGCCATCATCCCCACCC R TCCACAGTCCAGGAAAGACAGACCC	58	375
Zip14A[72]	F TTCCTCAGTGTCTCACTGATTAA R GGAAAAGGGCGTTAGAGAGC	54	142

Table 2.2: Real-Time PCR Cycling Parameters

Steps	Temperature (°C)	Time (seconds)	Number of Cycles
Initial Denaturation	95	300	1
Denaturation	95	15	40
Annealing	50 – 60	20	
Extension	72	20	
Hold	72	30	1
Melting Curve	72 – 99	5	1 per 1°C increment
Hold	40	30	1

In addition RT-PCR was used to screen LR reaction transformants and pGEM-T transformants to determine whether they contained the correct plasmid. The reaction was performed as described above with supernatant from the overnight culture (Section 2.4.9.3) using qF1/qR1 primers for the LR reaction and qF2/qR2 and qF3/qR3 primers for the pGEM-T reaction (Table 2.1).

2.4.6 Polymerase Chain Reaction of cDNA and Plasmids

PCR was performed on cDNA from RNA extracted from wild-type mouse liver tissue for the purpose of creating expression clones and to generate plasmid standards. In addition PCR was used to screen transformed colonies and confirm the existence of the plasmid. All reactions were carried out in 0.2 mL low adhesion nuclease free tubes in 20 µL reactions in a PTC-100TM thermal cycler.

2.4.6.1 Polymerase Chain Reaction of *ZnT-1* Coding Sequence for Cloning

Forward and reverse primers were designed using the a web-based computer programme Primer 3[65] with *att*B sites to facilitate cloning into a Gateway® vector

Primers were designed by Ross Graham to amplify the *ZnT-1* coding sequence. They included four guanine (G) residues at the 5' end followed by a 25 base sequence known as the *att*B1 site and *att*B2 site (underlined) for forward and reverse primers respectively, followed by 20 base gene-specific sequences. Furthermore two additional nucleotides were included (highlighted) to maintain the proper reading frame with the *att*B1 region once the PCR product was fused in frame with an N-terminal tag. In addition shorter primers were designed without *att*B sites (Table 2.3).

Table 2.3: Primers used for PCR of *ZnT-1*

Primer	**Primer Sequence (5' – 3')**	**Product Size**
cF cR	GGGGACAAGTTTGTACAAAAAAGCAGGCTTC ATGGGCTGCTGGGGCCGCAA GGGGACCACTTTGTACAAGAAAGCTGGGTC CTCACAAAATGATTCGGGC	1574
cFsh1 cRsh	ATGGGCTGCTGG GGCCGCA CTCACAAAGATGATTCGGGC	1513
cFsh2	GCTTCGGTCCGATGCTC (use with cRsh1)	1676

To determine the optimal conditions for the reaction it was necessary to undertake several PCR reactions to optimise conditions such as DNA Polymerases, Mg^{2+} and primer concentrations and PCR enhancing agents such as PCR enhancer, Q Solution, DMSO and Glycerol. PCR enhancers can facilitate efficient amplification of problematic templates or GC-rich sequences, Q Solution changes the melting behaviour of DNA[73], and DMSO and Glycerol not only lower the

primer and template melting temperature (T_M) but also aid in relaxing GC secondary structures[74; 75].

Generally, for all reactions, a master mix was prepared containing 0.2 mM – 2 mM dNTPs, 0.25 µM – 4 µM of each forward and reverse primer, 2 mM – 3 mM Mg^{2+}, 0.5 – 5 U DNA Polymerase, 1x reaction buffer and plus or minus one or more of the abovementioned PCR enhancing agents in nuclease free water to a final volume of 17.5 µL to 19 µL per sample and aliquoted into tubes to which 1 µL – 2.5 µL of cDNA was added. All reactions underwent PCR according to the cycling parameters listed in Table 2.4. In each instance cycling parameters and the addition and concentration of reagents and enhancers was determined from results of the preceding reaction as well as in accordance with reagent specifications.

Ultimately *ZnT-1* was amplified using 0.6 mM dNTPs, 0.25 µM of each forward and reverse primer, 2 mM Mg^{2+}, 1x reaction buffer, 1x PCR enhancer, 5% DMSO, 5 units *Pfx50* and 2 µL cDNA and were subjected to an initial denaturation cycle (94°C, 2 min) followed by 35 cycles of denaturation (94°C, 30 s); annealing (54°C, 30 s); and extension (68°C, 100 s) before a final 5 min extension step at 68°C and holding at 4°C.

Table 2.4: PCR Cycling Parameters

Steps	Temperature (°C)	Time (seconds)	Number of Cycles
Initial Denaturation	94 – 95	120	1
Denaturation	94 – 95	30	35
Annealing	50 – 68	30	
Extension	68 – 72	90 – 100	
Final Extension	68 – 72	300 – 600	1
Hold	4	∞	1

2.4.6.2. Polymerase Chain Reaction of *ZnT-1* for Plasmid Standards

PCR was also used to amplify a fragment of the *ZnT-1* gene to create plasmid standards to be used in RT-PCR. Two sets of primers were used to amplify regions specific to different mRNA isoforms qF2/qR2 and qF3/qR3 (Figure 2.1; Table 2.1). A master mix was prepared as described in Section 2.4.5 without 1x SYBR. Samples were then subjected to an initial denaturation cycle (94°C, 2 min) followed by 35 cycles of denaturation (94°C, 30 s); annealing (58°C, 30 s); and extension (72°C, 1 min) before a final 2 min extension step at 72°C and holding at 4°C.

In addition PCR was used to screen BP and LR reaction transformants (Section 2.4.9.1; 2.4.9.3) in order to determine whether they contained the correct plasmid. Primers used were cF/cR and cFsh1/cRsh for BP and LR transformants respectively. A master mix was prepared as described in Section 2.4.5 with the following exceptions: 2.5 mM $MgCl_2$, 1x PCR Enhancer, 5% DMSO and 1 µL of supernatant from the overnight culture (Section 2.4.9.1; 2.4.9.3) was added. Samples were then subjected to an initial denaturation cycle (94°C, 2 min) followed by 35 cycles of denaturation (94°C, 30 s); annealing (54°C, 30 s); and extension (72°C, 100 s) before a final 5 min extension step at 72°C and holding at 4°C.

2.4.7 Agarose Gel Electrophoresis of PCR Products

The procedure was performed as described in Section 2.4.3, however, 15 – 20 µL of the product was loaded into each well after mixing with 2 – 3 µL of 6x loading dye and electrophoresed for 40 min to 1 h.

2.4.8 Purification of PCR Products and Gel Extraction

The PCR products were prepared for cloning by purifying the product or extracting and purifying a band of the correct size cut from an agarose gel. PCR purification was performed using the PureLink® PCR Purification Kit (Invitrogen) or the ChargeSwitch®-Pro PCR Clean-up Kit (Invitrogen) according to the manufacturer's instructions and gel extraction and purifications were performed using the QIAquick® Gel extraction Kit (QIAGEN) as per the manufacturer's instructions. Briefly, samples were added to a column along with a binding buffer and centrifuged (10,000*g*, 1 min) to allow the DNA to bind to the column. Addition of a wash buffer and further centrifugation (10,000*g*, 1 min) removed any contaminants after which the DNA was eluted in 50 µL buffer (20 mM Tris-HCl, pH 8.5). DNA concentrations were measured by spectrophotometry as previously described in Section 2.4.2

2.4.9 Cloning of *Znt-1* into Vectors

The purified ZnT-1 gene was cloned using Gateway® Technology (Invitrogen) vectors to create an expression clone. In addition, a fragment of *ZnT-1*, amplified as described in Section 2.4.6.2, was cloned into the pGEM®-T Easy Vector (Promega) to generate a plasmid standard.

The creation of an expression clone was achieved via a two-step cloning process; the BP Clonase and LR Clonase reactions generated entry clones and expression clones respectively.

2.4.9.1 Construction and Amplification of pENTR221-ZnT-1 Entry Clones

To create pENTR221-ZnT-1 the purified *att*B-*ZnT-1* product (103.88 ng) was combined with Gateway® pDONR221 vector (150 ng), 1.25x BP Clonase Reaction Buffer and TE Buffer (pH8.0) to a final volume of 8 µL. BP Clonase Enzyme was thawed on ice (2 min) and after vortexing (twice, 2 s) 2 µL was added to the reaction and allowed to incubate (25°C, 2 h). BP Clonase facilitates a recombination reaction between *att* sites on the interacting DNA molecules and the presence of the *ccd*B gene in the pDONR221 vector allows negative selection by inhibiting growth of *E. coli* carrying the pDONR221 vector or the by-product molecules retaining the *ccd*B gene[2] (Figure 2.2). The BP Clonase enzyme was then digested to prevent further recombination reactions by adding Proteinase K (2 µg) and incubating (37°C, 10 min) the reaction was either stored (-20°C) or used immediately to transform *E. coli* DH5-α.

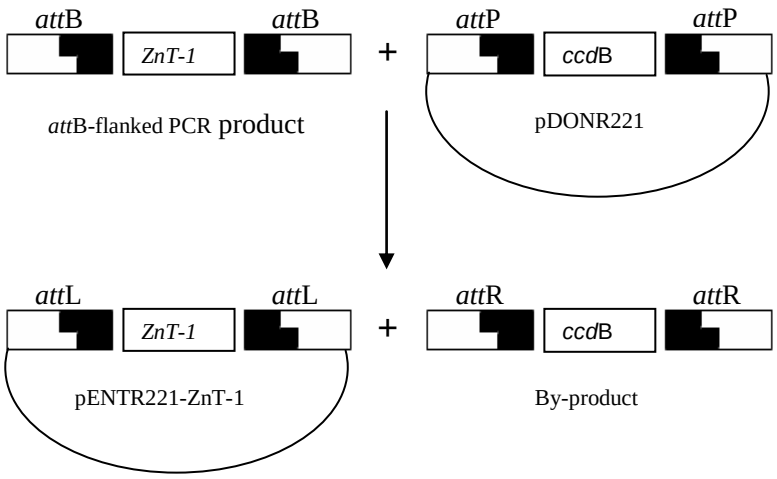

Figure 2.2: BP Reaction. Recombination between *att*B-flanked PCR product and Gateway® pDONR221 vector generates pENTR221-ZnT-1 adapted from Invitrogen[76].

A 1.5 µL aliquot of the BP Clonase recombination reaction was added to 100 µL of competent *E. coli* DH5-α cells and incubated for 30 min on ice. The cells were heat shocked (42°C, 30 s) and immediately transferred to ice before the addition of 900 µL SOC medium. After incubating with shaking (37°C, 1 h, 250 rpm) a glass spreader was used to spread 100 µL and 20 µL of the reaction onto LB agar plates containing kanamycin (50 µg/mL) to select the growth of colonies containing plasmids expressing the km-resistance gene. Following an overnight incubation at 37°C a single colony was picked from the plate with a disposable loop and used to inoculate both 10 µL of nuclease free water in a 1.5mL microcentrifuge tube and 8 mL LB containing kanamycin (50µg/mL). The sample was boiled (95 °C, 5 min) before centrifuging (10,000*g*, 1 min) and the supernatant used in a PCR reaction as described in Section 2.4.6. The products were analysed by agarose gel electrophoresis (Section 2.4.7) to verify if bacterial colonies contained the correct product.

The 8 mL LB was incubated overnight with shaking (37°C, 250 rpm) and pENTR221-ZnT-1 was extracted using the FastPlasmid™ Mini Kit (Eppendorf) or the QIAprep® Spin Miniprep Kit (QIAGEN) according to the manufacturer's instructions. Briefly, cells were lysed and after precipitating the protein the tubes were centrifuged (16,000*g*, 1 min) to pellet the denatured protein. The supernatant was added to the column allowing the DNA to bind and the DNA was washed with a solution containing 30% isopropanol to remove any remaining impurities before eluting in 50 µL buffer (10 mM Tris-HCl pH 8.0, 0.1 mM EDTA). pENTR221-ZnT-1 DNA concentration was quantitated by spectrophotometry, as previously described in Section 2.4.2 and stored at -20°C.

2.4.9.2 Sequencing of pENTR221-ZnT-1 Entry Clones

pENTR221-ZnT-1 entry clones were sequenced to definitively confirm the correct gene was cloned and determine whether the sequence was free from mutations. Two reactions, one forward and one reverse, were prepared by taking an aliquot containing 400 ng of plasmid and combining with nuclease free water to a final volume of 15 µL in a 1.5 mL microcentrifuge tube. The reactions were sent to The Gandel Charitable Trust Sequencing Centre, Monash Institute of Medical Research, Melbourne who carried out DNA sequencing with the M13 Fwd and "Reverse" primers using the Dideoxy method.

The chromatogram was reviewed using the CodonCode Aligner[77] computer programme and the forward and reverse DNA sequence files were aligned against the NCBI NM_009579.3 mRNA sequence using Sequence Analysis[78]. The complete coding sequence was determined by aligning the forward and reverse sequences and translated to the protein sequence using Sequence Analysis after which it was aligned against the NCBI NP_033605.1 protein sequence and checked for differences.

2.4.9.3 Construction of Expression Clones

The pcDNA/GW-N-EmGFP/ZnT-1 and pT-REx/GW/ZnT-1 expression clones were constructed by combining 300 ng of the pENTR221-ZnT-1 entry clone with 150 ng of Gateway® destination pcDNA6.2/N-EmGFP-Dest or pT-REx-DEST vectors respectively along with 1.25x LR Clonase Reaction Buffer and TE Buffer (pH8.0) to a final volume of 8 µL. LR Clonase Enzyme was thawed on ice (2 min) and after vortexing (twice, 2 s) 2 µL was added to the reactions and allowed to

incubate (25°C, 2 h). As per the BP reaction, the LR reaction uses a recombination reaction (Figure 2.3). To digest the LR Clonase enzyme and prevent further recombination reactions, Proteinase K (2 µg) was added and after incubating (37°C, 10 min) the reactions were either stored (4°C) or used immediately to transform *E. coli* DH5-α.

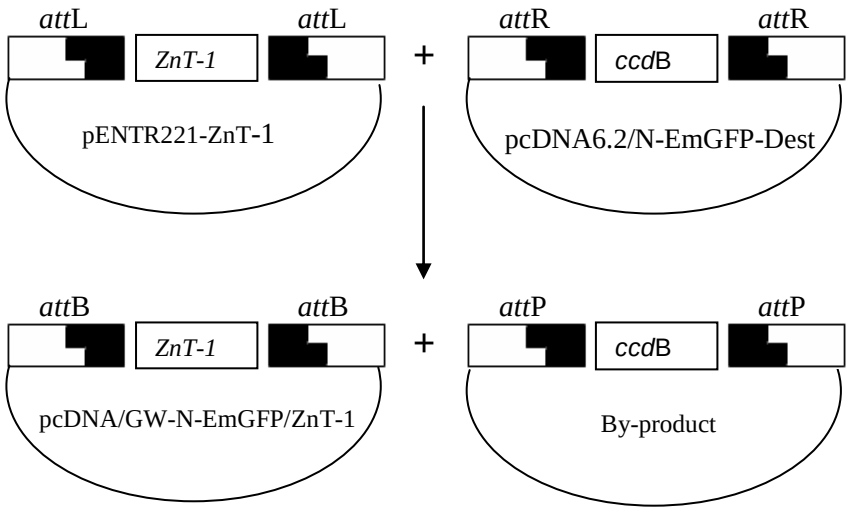

Figure 2.3: LR Reaction. Recombination between pENTR221-ZnT-1 and Gateway® pcDNA6.2/N-EmGFP-Dest vector generates pcDNA/GW-N-EmGFP/ZnT-1 adapted from Invitrogen[76].

A 1.5 µL aliquot of the LR Clonase recombination reactions were added to 100 µL of competent *E. coli* DH5-α cells in 1.5 mL microcentrifuge tubes and incubated for 30 min on ice. The cells were heat shocked (42°C, 30 s) and immediately transferred to ice before the addition of 900 µL SOC medium. After incubating with shaking (37°C, 1 h, 250 rpm) a glass spreader was used to spread 100 µL or 20 µL of the reactions on to LB agar plates containing ampicillin (100µg/mL) to ensure the growth of colonies containing plasmids expressing the amp-resistance gene. Following an overnight incubation at 37°C a single colony was picked from the plate with a disposable loop and used to inoculate both 10 µL

of nuclease free water in a 1.5mL microcentrifuge tube and 8 mL LB containing ampicillin (100 µg/mL). The sample was boiled (95 °C, 5 min) before centrifuging (10,000*g*, 1 min) and the supernatants used in RT-PCR and PCR reactions as described in Sections 2.4.5 and 2.4.6. For RT-PCR reactions, the melt curve was analysed to verify amplification of a single product and for PCR reactions the products were screened by agarose gel electrophoresis (Section 2.4.7) to verify that bacterial colonies contained the correct sized product.

After an overnight incubation with shaking (37°C, 250 rpm) the pcDNA/GW-N-EmGFP/ZnT-1 and pT-REx/GW/ZnT-1 plasmids were extracted using the FastPlasmid™ Mini Kit (Eppendorf) or the QIAprep® Spin Miniprep Kit (QIAGEN) according to the manufacturer's instructions as described in Section 2.4.9.1. The concentration was quantitated by spectrophotometry as previously described in Section 2.4.2 and pcDNA/GW-N-EmGFP/ZnT-1 and pT-REx/GW/ZnT-1 were stored at -20°C.

pcDNA/GW-N-EmGFP/ZnT-1 and pT-REx/GW/ZnT-1 was used to transform *E. coli* DH5-α as previously described (Section 2.4.9.3), spread on LB plates containing ampicillin (100 µg/mL), incubated overnight (37°C) and starter cultures were prepared by inoculating 4 mL LB containing ampicillin (100 µg/mL). After an 8 h incubation period (37°C, 250 rpm) the cultures were expanded by inoculating 200 mL LB containing ampicillin (100 µg/mL) with 400 µL of the starter culture (1:1000 dilution) and incubated with shaking (37°C, 250 rpm, 12 h). A RT-PCR was performed (Section 2.4.5), using supernatant derived

from the starter cultures and the melt curve was analysed to screen for pcDNA/GW-N-EmGFP/ZnT-1 and pT-REx/GW/ZnT-1.

Following incubation pcDNA/GW-N-EmGFP/ZnT-1 and pT-REx/GW/ZnT-1 were extracted and purified using the PureLink™HiPure Plasmid Filter Purification Kit (Invitrogen) according to the manufacturer's instructions. In brief, cells were lysed and after precipitating the protein (Potassium acetate solution) the lysate was loaded on to an anion-exchange column allowing the DNA to bind. The DNA was washed with a sodium acetate/NaCl solution to remove any remaining impurities before eluting by gravity flow under high salt conditions with 15 mL of buffer. The DNA was precipitated with isopropanol (15,000*g*, 30 min, 4°C) and washed with 70% ethanol (15,000*g*, 5 min, 4°C) after which the pellet was air dried and resuspended in 500 µL TE Buffer (10mM Tris-HCl pH 8.0, 0.1mM EDTA). The concentration was quantitated by spectrophotometry (Section 2.4.2) and pcDNA/GW-N-EmGFP/ZnT-1 and pT-REx/GW/ZnT-1 were stored at -20°C. In addition glycerol stocks was prepared by pelleting 3 mL of the culture (3,000*g*, 5 min), resuspending it in 25% glycerol (1 mL 75% LB, 25% glycerol, 100 µg/mL ampicillin) and storing at -80°C.

2.4.9.4 Generation of Plasmid Standards

To create plasmid standards for RT-PCR of the SUI and LUI isoforms a fragment of *ZnT-1* corresponding to each of the isoforms was cloned into pGEM-T (Promega). 10.5 ng and 11.75 ng of the purified SUI and LUI PCR product was combined with pGEM®-T Easy Vector (50 ng), 1x Rapid Ligation Buffer, and 5U T4 DNA Ligase to a final volume of 10 µL and incubated at 4°C. After an

overnight incubation a 2 µL aliquot of each reaction was added to a 1.5 mL microcentrifuge tube on ice to which 50 µL of *E. coli* DH5-α was added. The reactions were mixed gently and incubated on ice (20 min) before being heat shocked (42°C, 50 s) and immediately returned to ice for 2 min. 950 µL of SOC was added to each reaction and after 90 min incubation with shaking (37°C, 150 rpm) 100 µL of each reaction was spread on LB plates containing ampicillin (100 µg/mL), X-gal (1 mg) and IPTG (10 µM). The plates were incubated overnight at 37°C and a single colony was picked from the plate and grown overnight (37°C, 200 rpm) in 5 mL LB containing ampicillin (100 µg/mL). Plasmids were then extracted using the FastPlasmid™ Mini Kit (Eppendorf) according the manufacturer's instructions as briefly described in Section 2.4.9.1). A RT-PCR was carried out (Section 2.4.5.) at the same time using supernatant derived from the overnight culture as previously described. In order to confirm the plasmid was correct the melt curve was examined and PCR products were analysed by agarose gel electrophoresis as described in Section 2.4.7.

A 100 µL aliquot of the overnight culture was diluted (1:500) in 50 mL LB containing ampicillin (100 µg/mL) and incubated (37°C, 300 rpm). Following an overnight incubation the plasmids were extracted using the QIAGEN® Plasmid Purification Kit (QIAGEN) as per the manufacturer's instructions. Briefly, cells were lysed and after precipitating the protein the tubes were centrifuged (20,000*g*, 30 min, 4°C) and (20,000*g*, 15 min, 4°C) to pellet the protein. The supernatant was applied to the QIAGEN-tip allowing binding of plasmid DNA to the anion-exchange resin by gravity flow after which the DNA was washed (1 M NaCl; 50 mM MOPS, pH 7; 15% isopropanol) to remove any remaining impurities before

eluting by gravity flow with 5 mL buffer (1.25 M NaCl; 50 mM Tris-Cl, pH 8.5; 15% isopropanol) after which the DNA was precipitated with isopropanol (15,000*g*, 30 min, 4°C) and washed with 70% ethanol (15,000*g*, 10 min, 4°C). The pellet was allowed to air dry before being resuspended in 100 µL TE Buffer (10 mM Tris-HCl pH 8.0, 0.1 mM EDTA). The concentration was quantitated by spectrophotometry, as previously described and plasmid standards were generated by preparing a serial dilution of known copy numbers by calculating mass of plasmid (ng) in 10^{11} copies where 1 µg of 1000 bp DNA (plasmid + insert) = 1.52pmol. Plasmid DNA was stored at -20°C. In addition a glycerol stock was prepared as previously described and stored at -80°C.

2.4.10 Cell Culture of AML12 Cells

AML12 cells were subcultured when they reached approximately 80% confluency. Medium was aspirated from the tissue culture flask and the cells were washed with 10 mL PBS to remove traces of serum which contains trypsin inhibitor. The cells were incubated at 37°C with 2 mL of Trypsin-EDTA until they detached from the flask. 10 mL medium was added to neutralise the trypsin and the cell suspension was transferred to a 15 mL tube and centrifuged at room temperature (300*g*, 3 min). The pellet was resuspended in 1 mL of medium using a syringe and needle to separate the clumps of cells and an additional 9 mL of medium was added to the flask. The cell suspension was mixed by inverting and a cell count was performed using a haemocytometer. 8.0 x 10^5 cells were subcultured in to a sterile 75 cm^2 tissue culture flask containing 10 mL cell culture medium containing gentamicin and incubated at 37°C in 5% CO_2/95 % O_2 cell incubator. Medium was replaced on day four and cells were subcultured

into new 75 cm^2 flasks every seven days. In addition, cells were seeded into 6 or 12 well plates at a density of 3.5 x 10^5 in 1 mL of medium and 7.5 x 10^5 cells per well in 2 ml of medium for 6 and 12 well plates respectively and allowed to incubate at 37°C for 24 hours.

2.4.11 Transfection of AML12 Cells

AML12 cells were transfected with pcDNA/GW-N-EmGFP/ZnT-1 to produce a GFP fusion protein. In addition, untransfected cells or cells transfected with the GFP vector or pT-REx/GW/ZnT-1 were used as controls. Transfected cells will be referred to as GFP/ZnT-1, GFP and REx/ZnT-1 cells for AML12 cells transfected with pcDNA/GW-N-EmGFP/ZnT-1, GFP vector and pT-REx/GW/ZnT-1 respectively, and untransfected cells, simply as AML12 cells hereafter.

After a 24 hour period cells in 6 and 12 well plates were approximately 80% confluent and transient transfections were carried out using Lipofectamine™ and PLUS™ Reagents (Invitrogen) according to the manufacturer's recommendations. 1 µg of plasmid DNA was diluted for every 100 µL of OptiMEM and after mixing thoroughly 7.5 µL or 3 µL of PLUS™ reagent was added per well in 6 or 12 well plates, respectively. The reaction was mixed gently and left to incubate for 5 min at room temperature. Lipofectamine™ LTX reagent was mixed gently and 12.5 µL or 5 µL was added per well in 6 or 12 well plates, respectively and mixed thoroughly before a 30 min incubation at room temperature. Then, 500 µL or 200 µL of DNA-Lipofectamine™ LTX complex was added to each well of a 6 or 12 well plate respectively in a drop wise fashion, and rocked gently to mix before

incubating at 37°C for 6 hours after which the medium was replaced and the cells were incubated for a further 42 hours.

2.4.12 Extraction of RNA from cells

RNA was extracted from untransfected AML12 cells and AML12 cells transfected with pcDNA/GW-N-EmGFP/ZnT-1, GFP vector or pT-REx/GW/ZnT-1. After washing the cells with 2 mL PBS, 300 µL of cold TRI Reagent was added to each well, mixed immediately and left to incubate for 10 min at RT. The cells were lysed by pipetting and then transferred to a 0.6 mL microcentrifuge tube and incubated for 5 min at RT. After the addition of 30 µL of BCP the tubes were vigorously shaken for 30 s before incubating for a further 10 min at RT. The tubes were centrifuged (16000*g*; 15 min; 4°C) and the aqueous phase containing RNA was transferred to a 1.5 mL low adhesion microcentrifuge tube. An equal volume of isopropanol was added to precipitate the RNA and the tube was mixed by inverting. Following incubation (10 min; RT) the tube was centrifuged (16000*g*; 5 min; 4°C) to precipitate the RNA and the supernatant was removed. The RNA pellet was washed with 200 µL 75% ethanol, dislodged and centrifuged (8000*g*; 5 min; 4°C). The supernatant was removed and the pellet air dried before dissolving in 15 µL of nuclease free water (15 min; 55°C).

2.4.13 Fluorescence Microscopy

Fluorescence microscopy was undertaken to determine the cellular location of the ZnT-1 protein. Three wells of a 12 well plate containing AML12 cells were transfected with pcDNA/GW-N-EmGFP/ZnT-1 or GFP vector alone as previously described (Section 2.4.11) and incubated for 24 hours. GFP/ZnT-1 and GFP cells

were transferred to the wells of a chamber slide. The medium was removed from each well of the 12 well plate and the cells were washed with 1 mL PBS before adding Trypsin-EDTA to remove the cells from the plate. 1 mL medium was added to each well and transferred to a microcentrifuge tube. After centrifugation (700*g*, 3 min) the supernatant was removed and a further 1 mL of medium containing gentamicin (160 ng) was added. After using a syringe to remove clumps, 100 µL of the cell suspension was added to wells of the chamber slide and distributed evenly by gently rocking. The cells were incubated at 37°C for 24 hours after which the medium was removed and the cells were washed twice with 1 ml of cold PBS. 1 mL of ice cold acetone:methanol (1:1) was added to the wells to fix the cells and after incubating (4°C, 20 min) the cells were washed twice with 1 mL cold PBS before removing the chambers and allowing the slide to air dry. A cover slip was mounted using a drop of Prolong® Gold antifade reagent with DAPI.

The GFP/ZnT-1 and GFP cells were visualised on an Eclipse TE2000-U Microscope using DAPI and GFP/Alexa Fluor 488 excitation filters of 330 – 380 nm and 450 – 490 nm respectively and images were captured with a Nikon DS – L1 Camera.

2.4.14 Protein Extraction

AML12, GFP/ZnT-1 and GFP cells were washed with 1 mL PBS after which a further 1 mL was added to each well and a cell scraper was used to remove the cells. Replicate wells were pooled into 1.5 mL microcentrifuge tubes, centrifuged (10,000*g*, 5 min) and the supernatant removed. 100 µL of SDS Lysis Buffer was

added to each tube and the pellet was resuspended before sonication (3.2 mm probe; 15 s; 40V). After centrifugation (16,000*g*, 20 min, 4°C) the supernatant was transferred to clean low adhesion microcentrifuge tubes and stored at 4°C (short term) or -80°C (long term).

2.4.15 Quantification of Protein

Extracted protein was quantified using the Pierce Bicinchoninic Acid (BCA) Protein Assay Kit (Progen) which is based on the reduction of Cu^{2+} to Cu^{1+} by protein in the presence of an alkaline medium, and the chelation of Cu^{1+} by the BCA-containing reagent which forms a coloured product. The reaction was carried out according to the manufacturer's instructions. Briefly, BSA (2 mg/mL) was used as the protein standard and was diluted with Triton/NaOH to final concentrations of 0 – 500 µg/mL. Protein samples were diluted 1:39 with Triton/NaOH. 20 µL of each standard or sample was added to wells of a 96 well plate followed by the addition of 200 µL working reagent (1:50 solution containing colour reagents B and A). Following 1 hour incubation at 37°C, absorbance was measured on a FLUOstar Optima Microplate Reader at a wavelength of 570 nm.

2.4.16 Western Blot Analysis of Protein

50 µg of each protein was transferred to 0.6 mL low adhesion nuclease free tubes with 3.75 µL 4x sample buffer and nuclease free H_2O to a final volume of 15 µL. The samples were heated at 95°C for 5 min to inactivate proteases and denature proteins and briefly centrifuged (10,000*g*, 10 s) to mix contents.

ZnT-1 was detected using a NuPAGE® 4-12% Bis-Tris pre-cast gel according to the manufacturer's instructions (Invitrogen). Briefly, the gel was rinsed with Milli-Q H_2O and the comb removed before rinsing the sample wells. After positioning the gel in the QuickPoint™ Electrophoresis Cell, the inner buffer chamber was filled with 1x MOPS SDS Running Buffer (Invitrogen) until the wells were submerged.

10 µL of Molecular Weight Marker (5 µL MagicMark™ XP Western Standard; 5 µL Novex Sharp Protein Standard) was loaded into the first well. 15 µL of each protein sample was loaded into the remaining wells and the outer buffer chamber was filled with 1x MOPS SDS Running Buffer. The samples were electrophoresed at 200 V for approximately 1 hour until the dye had migrated to the bottom of the gel.

Following electrophoresis the gels were removed from the cell. Three filter papers pre-soaked in transfer buffer were arranged on the cathode of a transfer block followed by the gel, a nitrocellulose blotting membrane (Fisher Biotec) pre-soaked in transfer buffer and a further three pre-soaked filter papers (Figure 2.1). The anode was placed on top of the stack and the proteins were transferred onto the membrane for 1 hour at 280 mA.

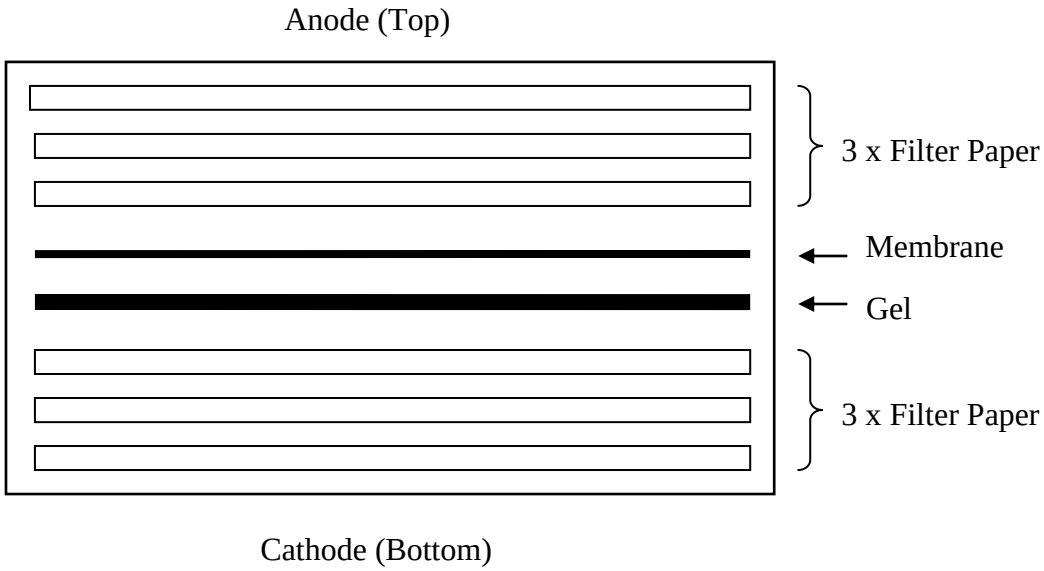

Figure 2.1: Semi-Dry Transfer Assembly Stack

Upon completion, the transfer stack was disassembled and the gel stained with Coomassie blue dye for a minimum of 30 min and de-stained in Milli-Q H_2O to confirm transfer of proteins. At the same time, the membrane was soaked in a 5% blocking solution for 30 min with agitation followed three brief rinses in PBS.

2.4.16.1 Detection of ß-Actin, ZnT-1/GFP, and GFP

Initially ß-Actin was detected by incubating the membrane with 5 mL of primary antibody (Section 2.2.5) overnight at 4°C with agitation after which the membrane was rinsed three times with PBS followed by a wash for 5 min with agitation. After repeating the rinse process twice, the membrane was incubated with 5 mL of secondary antibody (Section 2.2.5). After 1 hour incubation at room temperature with agitation, the membrane was rinsed three times with PBS followed by a wash for 5 min with agitation as described above. Detection was achieved by chemiluminescence using the Western Lightning™ *Plus*-ECL Detection Kit (Perkin Elmer) according to the manufacturer's instructions. Briefly, the

membrane was positioned on a transparent sheet on the VersaDoc Imaging system 3000 platform. After combining 2 mL each of Enhanced Luminol Reagent *Plus* and Oxidising Reagent *Plus* the solution was poured over the entire surface of the membrane and exposed for 300 s allowing a number of images to be captured.

The membrane was washed three times in PBS before carrying out a second incubation/wash/incubation process with primary and secondary antibodies (Section 2.2.5) to detect GFP.

2.4.17 Iron and Zinc Uptake/Release Assays

Iron and zinc transport was examined by incubating GFP/ZnT-1 and GFP cells with radiolabelled iron or zinc.

To test which form of zinc was most efficiently taken up, AML12 cells were incubated with either $^{65}ZnCl_2$ (1 µM) or ^{65}Zn citrate (1 µM). In addition, DTPA was examined for its effectiveness to chelate zinc. Subsequent assays were conducted with ^{65}Zn citrate (10 µM) or ^{59}Fe citrate (10 µM) for uptake experiments with the addition of DTPA or DFO for zinc or iron release experiments respectively.

GFP/ZnT-1 and GFP cells were washed 3 times with warm HBSS and 0.4 mL ^{59}Fe citrate was added to each well. Following a 1 hour incubation at 37°C the cells were washed 5 times with cold HBSS and 0.4 mL of release medium (RT) containing DFO was added to each well. Cells were incubated at 37°C for between 15 min and 24 hours after which the release medium was collected and

the cells were washed 5 times with cold HBSS. 800 µL of Triton/NaOH was added to each well and incubated briefly and the cell lysates collected. The above procedure was repeated for zinc uptake and release. Cells were incubated in ^{65}Zn citrate followed by washing, incubation in release medium containing DTPA and a final washing step before the cells were lysed. In addition, standards were prepared with 50 µL ^{59}Fe citrate or ^{65}Zn citrate incubation solution.

^{59}Fe or ^{65}Zn were counted for gamma radiation in a Wallac Wizard 3" 1480 gamma Counter. Specific activity was determined for ^{59}Fe and ^{65}Zn standards. Protein concentration was measured on the cell lysates using BCA protein assay previously described in Section 2.4.15 with the exception that protein samples were not diluted.

The uptake and release of both iron and zinc, expressed as nmol metal/g protein were calculated from counts per minute values detected by the gamma counter, the specific activity of ^{59}Fe and ^{65}Zn standards (cpm/nmol) and the amount of protein (µg/mL).

2.4.18 Statistical Analysis

Results were analysed using Microsoft Excel and are expressed as means ± SD or SEM. Initial F-tests were carried out to establish the assumption of equal or unequal variances after which the appropriate unpaired t-tests were performed. A difference was statistically significant if $p < 0.05$.

Chapter 3

Results

Introduction

mRNA levels of the two *ZnT-1* isoforms as well as those of *Fpn, TfR1* and *Hamp* were measured to determine gene expression. Liver tissue collected from wild type, iron loaded and iron deficient mice as well as *Hfe* knockout, *TfR2*(Y245X) mutant and Hfe-/-/TfR2(Y245X) double mutant mouse models of haemochromatosis was analysed by RT-PCR.

PCR was carried out to amplify *ZnT-1* after which it was cloned using Gateway® Technology vectors to create the expression clone pcDNA/GW-N-EmGFP/ZnT-1 and control clone. In addition, fragments of *ZnT-1* were cloned into the pGEM®-T Easy Vector to generate standard curves for RT-PCR analysis.

AML12, a mouse hepatocyte line was cultured and transfected with the ZnT-1 expression clone or control GFP plasmid. Cells were visualised by fluorescence microscopy to determine ZnT-1 localization, and mRNA levels of *ZnT-1*, *Fpn*, *Dmt1* and *Zip14* were measured by RT-PCR. Furthermore, protein was extracted from the transfected and non-transfected cells and analysed by Western blotting. Additionally, transfected and non-transfected cells were incubated with radiolabelled zinc and iron to determine cellular uptake and release of the metals.

3.1 Generating a Standard Curve for Real-Time PCR

3.1.1 PCR of a *ZnT-1* Fragment to Generate a Standard Curve

PCR was carried out to amplify a fragment of the ZnT-1 gene to create plasmid standards to be used in RT-PCR (see Section 2.4.6.2). Two sets of primers, qF2/qR2 and qF3/qR3, were used to amplify the short and long untranslated regions producing 210 bp and 234 bp products, respectively (Figure 3.1).

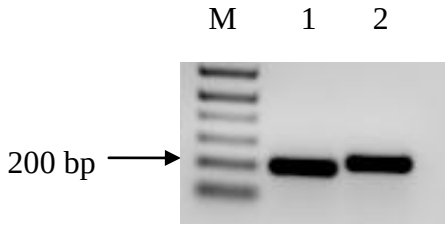

Figure 3.1: Agarose Gel showing *ZnT-1* fragments amplified by PCR. Lane M contains 1 Kb Plus Molecular Weight Marker and lane 1 and 2 contain *ZnT-1* fragments amplified from the short and long untranslated regions respectively.

3.1.2 Cloning of *ZnT-1* Fragments to Generate Standard Curves

ZnT-1 fragments were cloned into pGEM-T in order to generate standard curves for RT-PCR. Two fragments were amplified and subsequently cloned as described in Sections 2.4.6.2 and 2.4.9.4 after which RT-PCR (Section 2.4.5) was used to verify the presence of each insert. The melt peak shows that the SUI PCR products had the same melt temperature and that this was different from the melt temperature for the LUI PCR products (Figure 3.2).

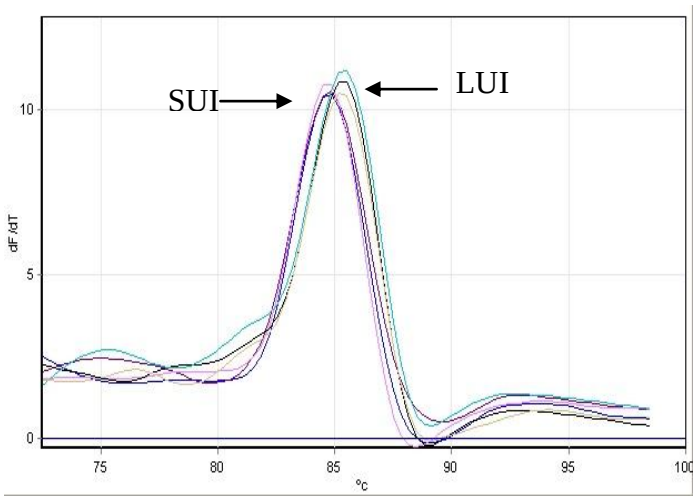

Figure 3.2: Melt Curves of *ZnT-1* Fragments. Melt Curve showing the different melt peaks generated for the SUI and LUI PCR products.

3.2 Real-Time Polymerase Chain Reaction

To analyse the role of ZnT-1 in iron transport, expression of *ZnT-1* was examined in wild type, iron loaded, iron deficient, *Hfe* knockout, *TfR2* mutant and double mutant mouse models by RT-PCR.

RNA was extracted from mouse liver as previously described (Section 2.4.1) and DNase treated to remove any remaining genomic DNA (Section 2.4.2). RNA integrity was examined by agarose gel electrophoresis to verify the presence of the 28S and 18S bands (Figure 3.3)

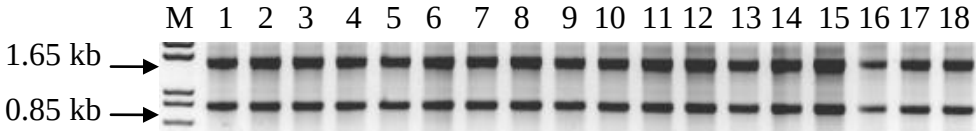

Figure 3.3: Representative Agarose Gel of RNA samples. RNA samples were electrophoresed on a 1.5% agarose gel. Lane M contains 1 Kb Plus Molecular Weight Marker, lanes 1- 9 contains RNA extracted from AML12 cells, lanes 10-18 contains RNA extracted from mouse liver.

Reverse transcription was carried out on RNA to generate cDNA after which samples were analysed by RT-PCR (Sections 2.4.4; 2.4.5). RT-PCR reactions were carried out to measure expression of genes in whole liver or a hepatocyte cell line.

RT-PCR uses fluorophores to detect levels of gene expression which correspond to the number of copies of mRNA of the gene of interest that exist for a particular gene. During amplification the exponential phase of the reaction was monitored using SYBR green, a fluorescent dye which binds to dsDNA, and increases exponentially in intensity with increasing number of cycles. A quantitation curve was generated which plots the fluorescence intensity versus the number of cycles on a semi-log graph. The threshold, on the quantitation curve, was used to calculate the CT values and give the line of best fit for the plasmid standard curve ($10^1 – 10^{10}$). The copy numbers for each sample were calculated from the plasmid standard curve and normalized to ß-actin.

After amplification, products were subjected to a melt cycle where the temperature increased in increments of 1°C from 72°C to 99°C. This identifies the peak melting temperature of the PCR product and is specific to each product[79].

The melt peak was analysed to verify the amplification of only a single product and this was confirmed by agarose gel electrophoresis and the product size was determined.

Figure 3.4 shows a representative quantitation curve (a), melt curve (b) and standard curve (c) with samples plotted in red.

(a)

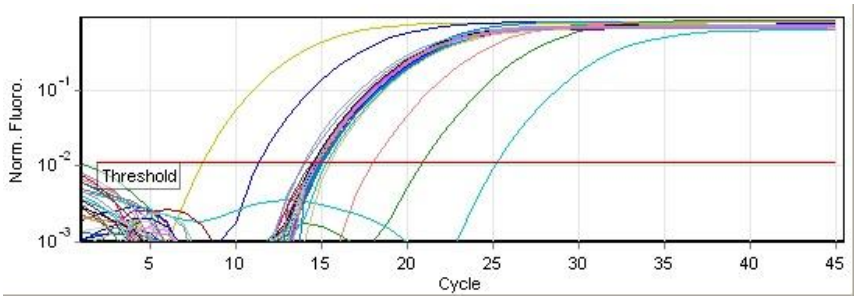

(b)

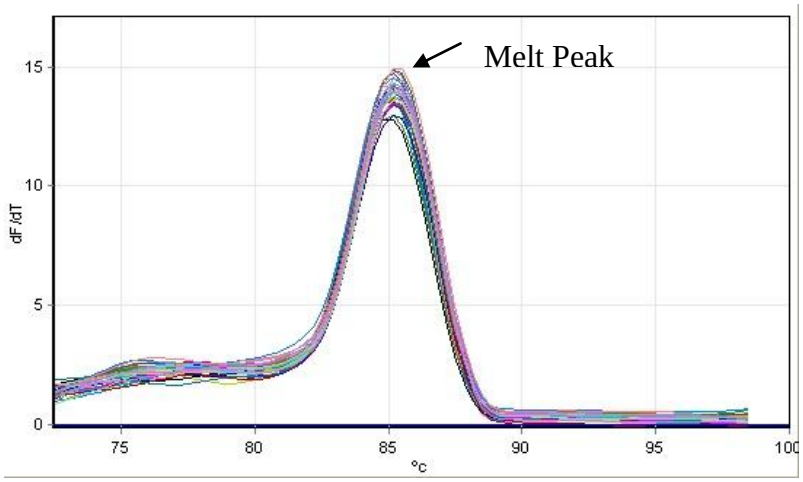

c)

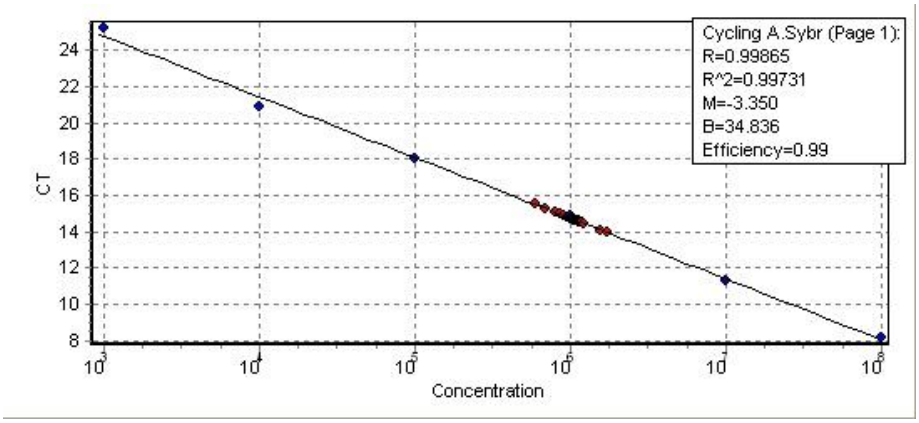

Figure 3.4: Representative Curves generated in RT-PCR. (a) **Quantitation curve** shows a semi-log graph of SYBR green fluorescence vs. cycle number. (b) **Melt curve** illustrate**s** the peak which is the specific melting temperature of the PCR product. (c) **Standard curve** shows the line of best fit generated from the CT values for increasing copy numbers of the standard plasmid (10^3 – 10^8; in blue) and the samples quantified from the standard curve (in red).

Figure 3.5 is a representative gel containing PCR products from RT-PCR.

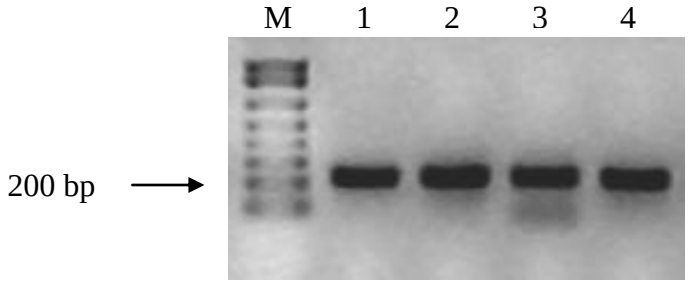

Figure 3.5: Representative Agarose Gel of RT-PCR products. Products were electrophoresed on a 1% agarose gel. Lane M contains 1 Kb Plus Molecular Weight Marker, lanes 1 – 4 contain PCR products from RT-PCR using ZnT-1 qF1/qR1 primers which amplified a 228 bp product from wild type, Hfe, TfR2 and iron loaded mouse liver tissue respectively.

3.2.1 Liver mRNA Expression

RT-PCR reactions were carried out to measure expression of the two *Znt-1* isoforms, *Fpn*, *TfR1* and *Hamp* in mouse liver.

Z*nT-1* (SUI)

mRNA expression of the SUI of *ZnT-1* was significantly lower in the double mutant mice compared to wild type mice (Figure 3.6). No other significant differences were observed.

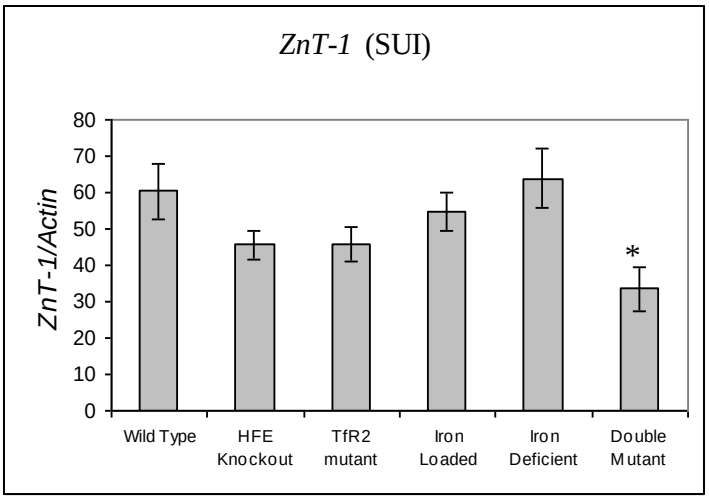

Figure 3.6: *ZnT-1* (SUI) liver mRNA expression in wild-type, *Hfe* Knockout, *TfR2* mutant, iron loaded, iron deficient and double mutant mice. Results are expressed relative to the housekeeping gene ß-actin as mean ± SEM, n = 6-8 (α = 0.05). *Significant differences were observed in double mutant mice compared to wild type mice ($p < 0.05$).

ZnT-1 (LUI)

In the LUI of *ZnT-1*, mRNA expression was significantly higher in the iron deficient mice than in the wild type mice (Figure 3.7). No other significant differences were observed.

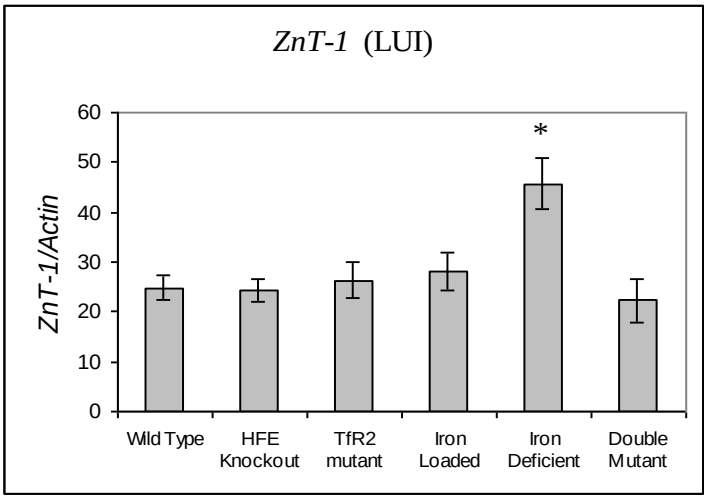

Figure 3.7: *ZnT-1* (LUI) liver mRNA expression in wild-type, *Hfe* Knockout, *TfR2* mutant, iron loaded, iron deficient and double mutant mice. Results are expressed relative to the housekeeping gene ß-actin as mean ± SEM, n = 6-8 (α = 0.05). *Significant differences were observed in iron deficient mice compared to wild type mice (p = 0.002).

Ferroportin

A significantly higher *Fpn* expression was observed in *Hfe* knockout, *TfR2* and iron loaded mice than in the wild type mice (Figure 3.8).

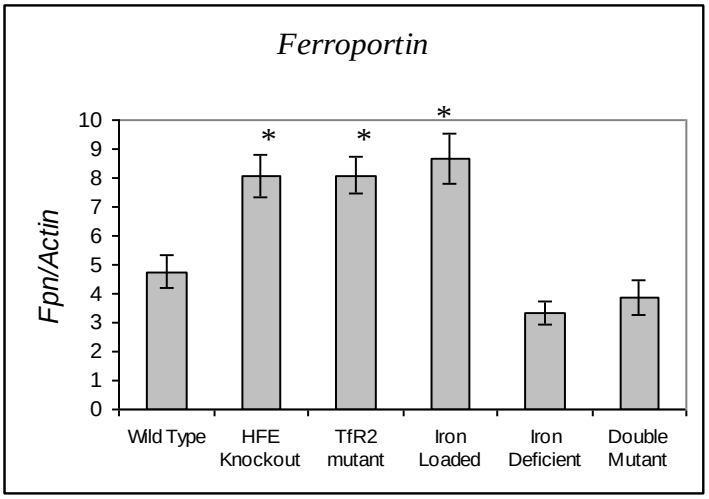

Figure 3.8: *Fpn* liver mRNA expression in wild-type, *Hfe* Knockout, *TfR2* mutant, iron loaded, iron deficient and double mutant mice. Results are expressed relative to the housekeeping gene ß-actin as mean ± SEM, n = 6-8 (α = 0.05). *Significant differences were observed in *Hfe* knockout, *TfR2*, and iron loaded mice compared to wild type mice (p < 0.005).

TfR1

TfR1 mRNA expression was significantly higher in iron deficient mice and significantly lower in double mutant mice compared to wild type mice (Figure 3.9).

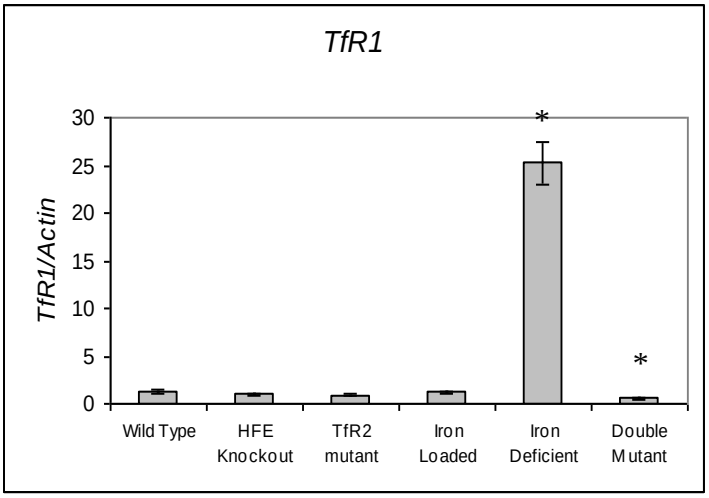

Figure 3.9: *TfR1* liver mRNA expression in wild-type, *Hfe* Knockout, *TfR2* mutant, iron loaded, iron deficient and double mutant mice. Results are expressed relative to the housekeeping gene ß-actin as mean ± SEM, n = 6-8 (α = 0.05). *Significant differences were observed in iron deficient ($p << 0.0001$) and double mutant mice compared to wild type mice ($p = 0.01$).

Hepcidin

mRNA expression of *Hepcidin* was significantly lower in *Hfe*, *TfR2*, iron deficient and double mutant mice than in wild type mice (Figure 3.10). In iron loaded mice, *hepcidin* expression was significantly higher than in wild type mice (Figure 3.10).

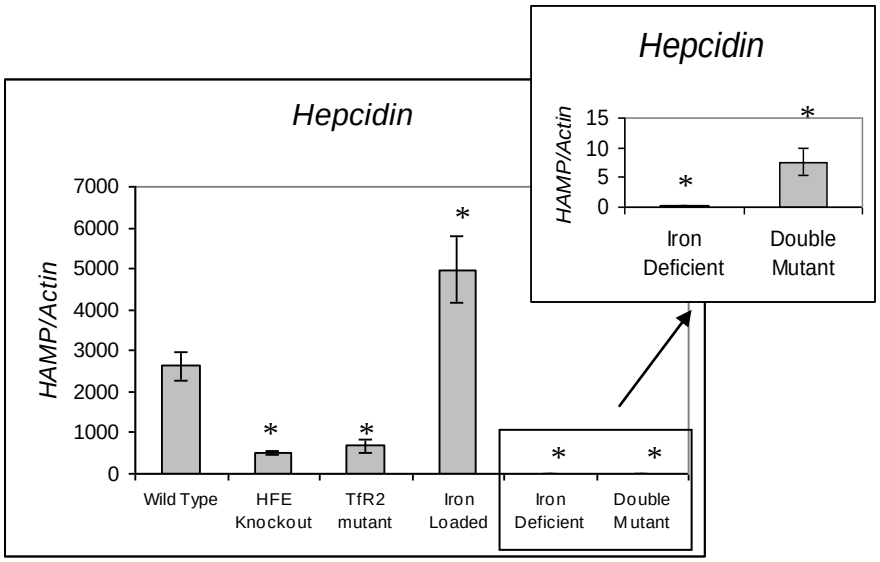

Figure 3.10: *Hepcidin* liver mRNA expression in wild-type, *Hfe* Knockout, *TfR2* mutant, iron loaded, iron deficient and double mutant mice. Results are expressed relative to the housekeeping gene ß-actin as mean ± SEM, n = 6-8 (α = 0.05).*Significant differences were observed in *Hfe* ($p < 0.001$), TfR2 ($p < 0.001$), iron loaded ($p < 0.05$), iron deficient ($p < 0.0005$) and double mutant mice ($p < 0.0005$) compared to wild type mice.

3.3 Cloning *ZnT-1*

3.3.1 PCR of *ZnT-1* Coding Sequence for Cloning

PCR was carried out using cDNA generated from RNA extracted from wild type mouse liver tissue as a template and *att*B primers to amplify the coding sequence of *ZnT-1* and generate a 1574 bp product (Section 2.4.6.1). Several reactions were required to optimise conditions before the product was successfully amplified. Conditions such as DNA Polymerases, Mg^{2+} and primer concentrations and PCR enhancing agents such as PCR enhancer and DMSO as well as annealing temperatures (T_A) were required to successfully amplify the sequence. However, once the product was cloned into Gateway® pDONR221 vector and the entry

clone was constructed, subsequent sequencing revealed mutations which resulted in two amino acid changes in a conserved region. Therefore, further PCR reactions were carried out using *Pfx50*™ DNA polymerase which has a higher proofreading ability (50 times improved fidelity) than *Taq* DNA polymerase[80]. Figure 3.11 shows a single band consistent with the expected size of 1574 bp.

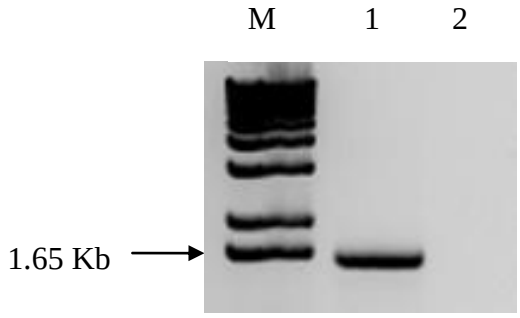

Figure 3.11: Agarose Gel of *att*B-*ZnT-1* PCR product amplified using *Pfx50* Polymerase. Lane M contains 1 Kb Plus Molecular Weight Marker and lane 1 contains the purified product and lane 2 is the –ve control which contains the master mix without template DNA indicating that there was no contamination.

In addition, another mutated clone was discovered which will be referred to as the short coding isoform (SCI) hereafter. The SCI was missing 269 nucleotides from the 5' end of the coding sequence which translated a 428 amino acid protein. A protein topology prediction in Geneious[81] revealed a five transmembrane protein with an extracellular carboxy terminus. Furthermore, the protein lacked the histidine-rich loop common to most zinc transporters. Unfortunately, due to time constraints, it was not possible to investigate this 'isoform' further.

3.3.2. Construction of Expression Clones

The construction of pcDNA/GW-N-EmGFP/ZnT-1 was achieved via a two-step cloning process. Initially, the entry clone pENTR221-ZnT-1 was created as described in 2.4.9.1 by cloning *att*B-*ZnT-1* into the Gateway® pDONR221 vector

and sequenced (Section 2.4.9.2). pcDNA/GW-N-EmGFP/ZnT-1 and pT-REx/GW/ZnT-1 were produced as described in Section 2.4.9.3 by cloning pENTR221-ZnT-1 into Gateway® pcDNA6.2/N-EmGFP-Dest and pT-REx-DEST destination vectors respectively.

To verify if bacterial colonies contained pENTR221-ZnT-1**,** a preliminary screening process was undertaken. PCR reactions as described in Section 2.4.6 were carried out on bacterial colonies transformed with the pENTR221-ZnT-1 recombinant to determine the presence and size of the product after which products were analysed by agarose gel electrophoresis. Samples in lanes 10, 13, 14, 15, 16 and 18 appear on the gel as one fragment consistent with the expected size of 1574 bp indicating the colonies contained pENTR221-ZnT-1 (Figure 3.12).

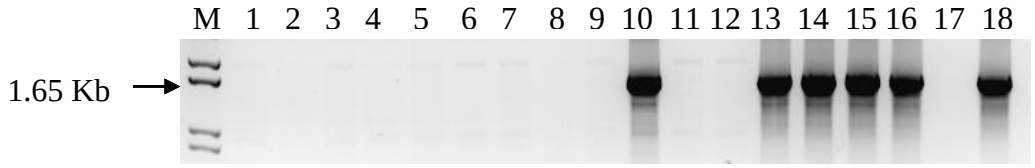

Figure 3.12: Agarose Gel of pENTR221-ZnT-1 PCR products amplified from bacterial colonies. Lane M contains 1 Kb Plus Molecular Weight Marker, lanes 1 – 9 contains PCR products amplified from bacterial colonies from the 20 µL plate and lanes 10-18 contains PCR products amplified from bacterial colonies from the 100 µL plates.

Consequently the six purified entry clones were submitted for sequencing to definitively confirm the correct gene was cloned and ensure it was free from mutations. After analysis as described in Section 2.4.9.2, three entry clones, from

colonies 13, 14 and 16 were confirmed as being mutation free *ZnT-1*. Figure 3.13 is a representation of the protein alignment of the three clones sequenced.

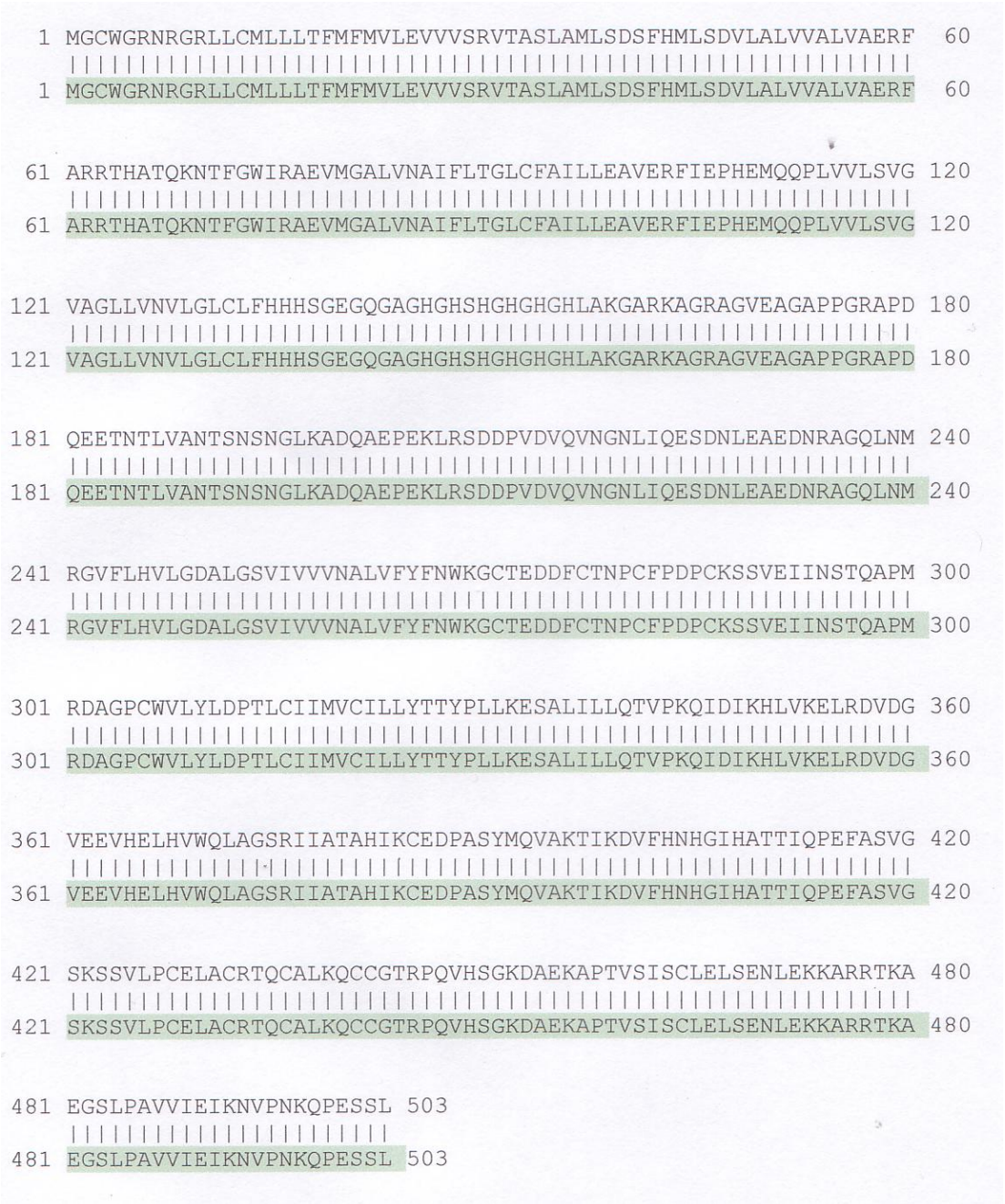

Figure 3.13: A representative amino acid sequence alignment. The image shows the amino acid sequence alignment for the plasmid derived from colony 13 and is representative of the three correct clones. The NCBI NP_033605.1[82] sequence is highlighted.

After sequencing revealed three pENTR221-ZnT-1 clones contained the ZnT-1 transcript, pcDNA/GW-N-EmGFP/ZnT-1 and pT-REx/GW/ZnT-1 were constructed and screened by both PCR and RT-PCR (Section 2.4.5; 2.4.6). Figure 3.14 shows that PCR products amplified from bacterial colonies transformed with the pcDNA/GW-N-EmGFP/ZnT-1 and pT-REx/GW/ZnT-1 recombinants were of the expected size of 1574 bp and analysis of the melt curve revealed the pcDNA/GW-N-EmGFP/ZnT-1 and pT-REx/GW/ZnT-1 PCR products had the same melt temperature.

(a)

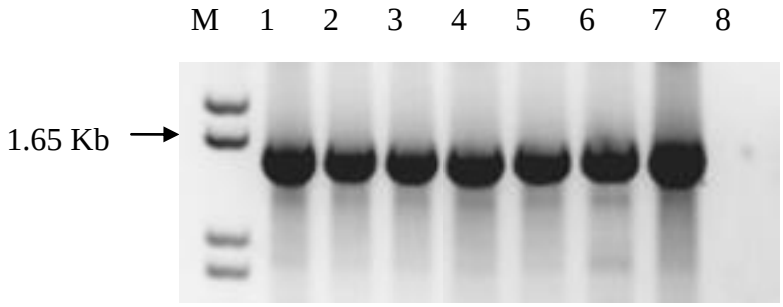

(b)

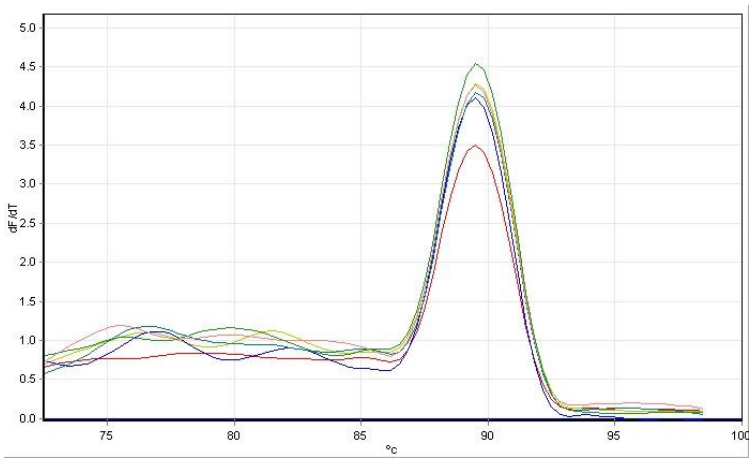

Figure 3.14 Agarose Gel and Melt Peak. (a) Agarose gel of pcDNA/GW-N-EmGFP/ZnT-1 and pT-REx/GW/ZnT-1 PCR products amplified from bacterial colonies. Lane M contains 1 Kb Plus Molecular Weight Marker, lanes 1 – 3 contain pcDNA/GW-N-EmGFP/ZnT-1, lanes 4 – 6 contain pT-REx/GW/ZnT-1, lane 7 contains the pENTR221-ZnT-1 clone from colony 14 as a +ve control and lane 8 contains the –ve control confirming there was no contamination. **(b) Melt Peak derived from RT-PCR of pcDNA/GW-N-EmGFP/ZnT-1 & pT-REx/GW/ZnT-1 amplification.** The melt curve showing all of the PCR products have the same melt temperature.

Therefore the expression clones were transformed (Section 2.4.9.3) using one pcDNA/GW-N-EmGFP/ZnT-1 clone and one pT-REx/GW/ZnT-1 clone, and after growing up in LB broth, an additional RT-PCR was carried out and the resulting melt curve for each clone showed the melt temperature was the same (Figure 3.15).

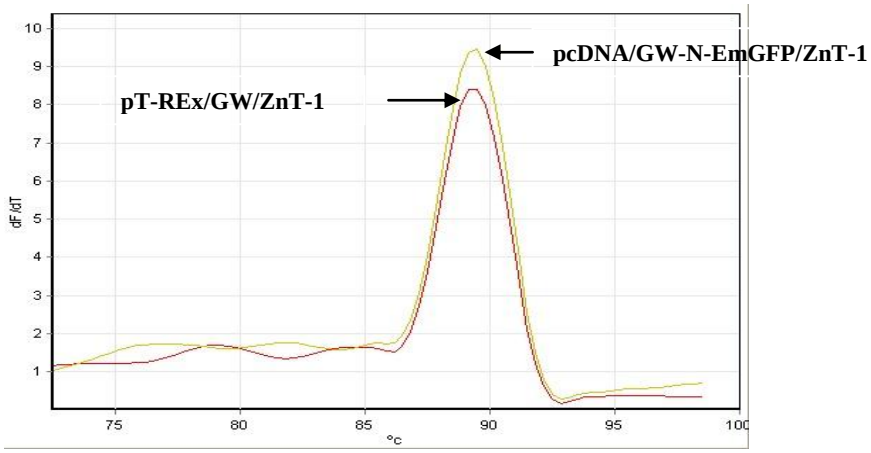

Figure 3.15: Melt Curve derived from RT-PCR of pcDNA/GW-N-EmGFP/ZnT-1 and pT-REx/GW/ZnT-1 starter culture. The melt curve shows a similar curve for pcDNA/GW-N-EmGFP/ZnT-1 and pT-REx/GW/ZnT-1.

3.4 Fluorescence Microscopy

Fluorescence microscopy was undertaken to determine the cellular location of the ZnT-1 protein (Section 2.4.13). GFP/ZnT-1 and GFP cells were fixed to a microscope slide and stained with Prolong® Gold antifade reagent containing DAPI. In GFP/ZnT-1 cells, green fluorescence (as indicated) was observed on the cell membrane (Figure 3.16a). In contrast, green fluorescence was observed on the cell membrane and intracellularly in GFP cells (Figure 3.16b). DAPI staining illustrated the nuclei (Figure 3.16c and d) and merging of the images illustrates expression of ZnT-1 on the cell membrane (Figure 3.16e and f). Furthermore, figure 3.16e shows some intracellular punctate staining.

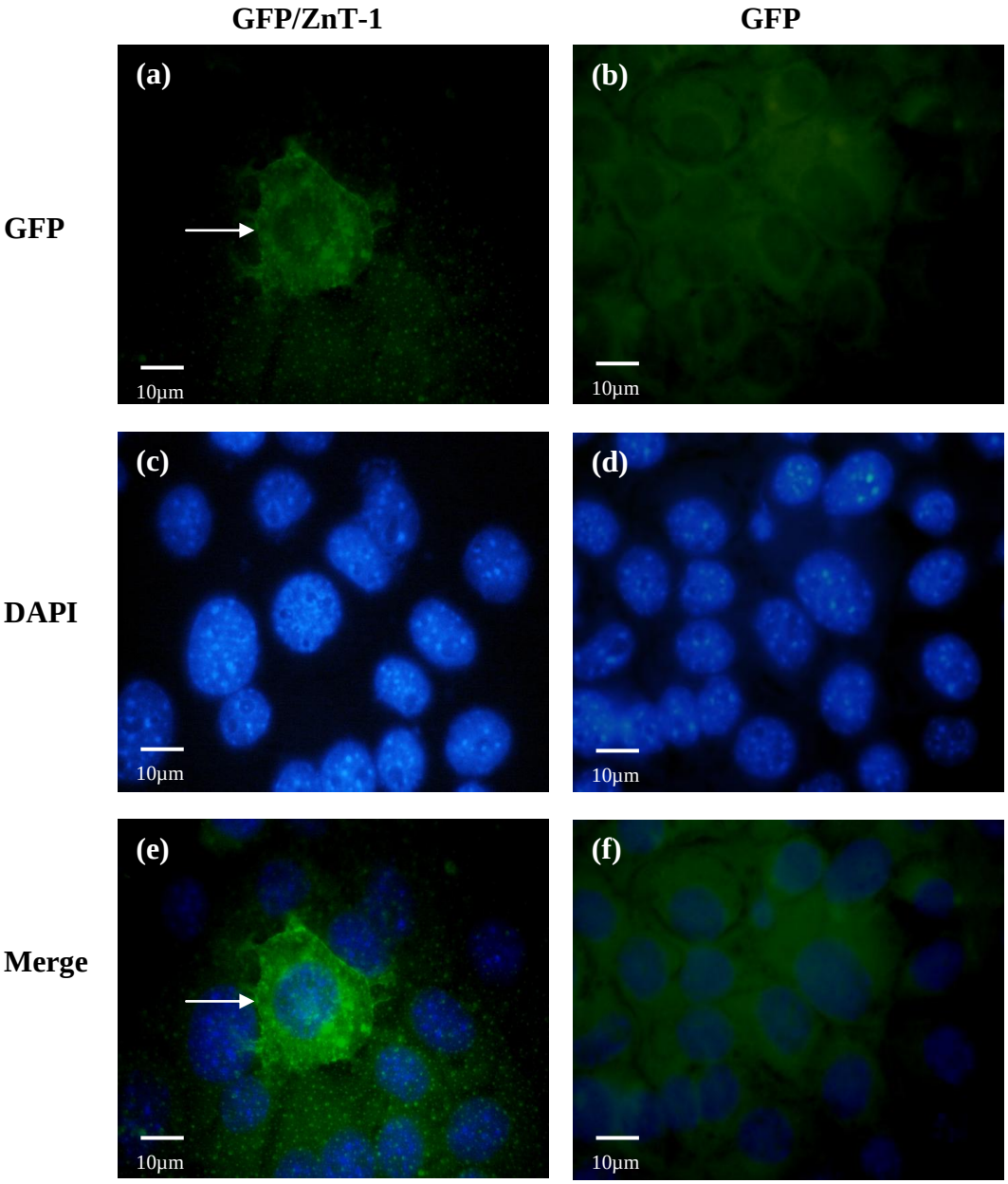

Figure 3.16: Fluorescent Images of AML12 Cells transfected with the GFP/ZnT-1 construct or GFP alone. (a) GFP/ZnT-1 cells show green fluorescence on the cell membrane as marked. (b) GFP cells show green fluorescence throughout the cell. (c) DAPI staining of GFP/ZnT-1 cells and (d) GFP cells illustrates the nuclei. (e) In GFP/ZnT-1 cells, the cells display intracellular punctate staining and expression is seen on the cell membrane as marked. (f) In GFP cells expression is shown throughout the cell.

3.5 Western Immunoblotting to detect the GFP protein

Total protein was extracted from AML12, GFP/ZnT-1 cells and GFP cells and quantitated (Section 2.4.14 and 2.4.15). GFP/ZnT-1 and GFP protein expression in AML12 cells was analysed by Western Blot as described in Section 2.4.16. GFP/ZnT-1 and GFP protein in AML12 cells was detected by using rabbit polyclonal GFP primary antibody and goat anti-Rabbit IgG horseradish peroxidase conjugate secondary antibody (Figure 3.17).

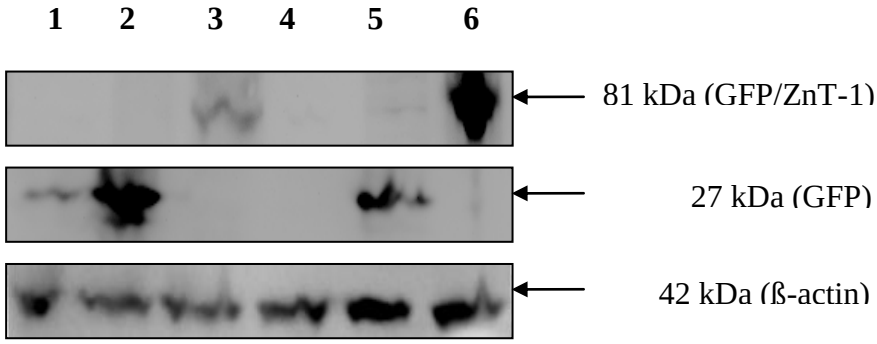

Figure 3.17: ZnT-1 Protein Expression. ZnT-1 protein levels were measured by Western Blotting by detecting the GFP in transfected AML12 cells. Bands specific for GFP/ZnT-1 are seen in lanes 3 and 6, GFP are in lanes 2 and 5 and ß-actin in lanes 1 – 6**.**

3.6 Iron and Zinc Uptake and Release Assays

To test which form of zinc was most efficiently taken up, AML12 cells were incubated with either $^{65}ZnCl_2$ or ^{65}Zn citrate. Furthermore, it was important to establish whether DTPA would be an effective zinc chelator to ensure that once released from the cell, zinc would not be taken up again (Section 2.4.17). Figure 3.18 shows that both $^{65}ZnCl_2$ and ^{65}Zn citrate were equally effective at donating zinc to the cells. In addition, the results show that when DTPA was added to the medium, uptake was significantly reduced thus it was concluded that DPTA is an

effective zinc chelator (Figure 3.18). Citrate and DFO are known to be efficient for uptake and release of iron respectively[83], and the use of these in iron assays is standard procedure in this laboratory. Therefore, to minimise the differences between assays, subsequent assays were performed with ^{65}Zn citrate or ^{59}Fe citrate for uptake and DTPA or DFO for release medium, for zinc and iron respectively.

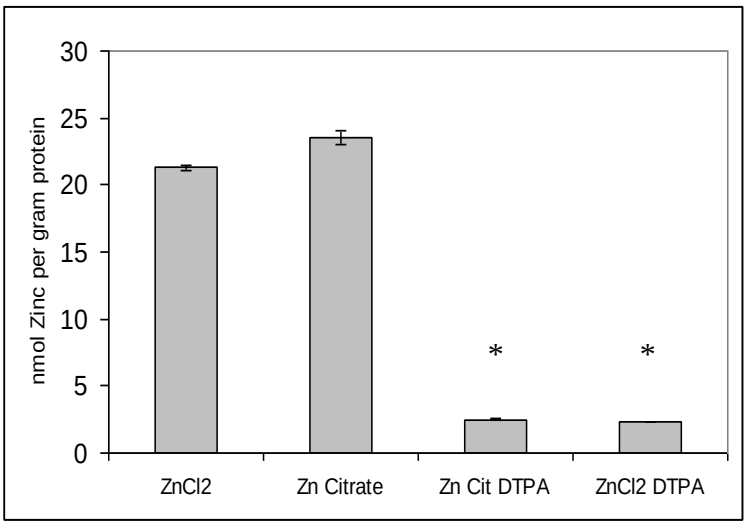

Figure 3.18: Uptake of $^{65}ZnCl_2$, ^{65}Zn Citrate, ^{65}Zn Citrate DTPA and $^{65}ZnCl_2$ DTPA in AML12 cells. Cells were incubated with $^{65}ZnCl_2$, ^{65}Zn Citrate, ^{65}Zn Citrate or $^{65}ZnCl_2$ DTPA (1µM Zn; 160nM Citrate; 100 µM DTPA) for 1 h at 37°C. Results are expressed as mean ± SE, n = 3 (α = 0.05). *Significant differences were observed in Zn Citrate DTPA and ZnCl2 DTPA uptake compared to both $^{65}ZnCl_2$ and ^{65}Zn Citrate ($p << 0.001$).

An efflux time course study was conducted to establish the optimum release time. Untransfected AML12 cells pre-incubated with ^{65}Zn Citrate or ^{59}Fe Citrate (37°C, 1 h) were washed and re-incubated in release medium containing DTPA (100 µM) or DFO (100 µM) for 15, 60, 120 and 240 min after which the release medium was collected and the amount of ^{59}Fe and ^{65}Zn was measured (Section 2.4.17). Iron and zinc released from the cell increased over the 240 min period. (Figure 3.19) Iron released in the first 60 min accounted for almost 90% of the total iron

released. There was a minimal amount of efflux over the next 180 min and at T_{240} about 85% of iron remained in the cell. A similar trend was observed for zinc where 75% of the total zinc released occurred in the first 60 min. Between T_{60} and T_{120}, the amount released was negligible; however, there was a significant amount of zinc released in the final 120 min and by T_{240} there was 70% of zinc remaining in the cell (Figure 3.19). More zinc than iron was released from the cell.

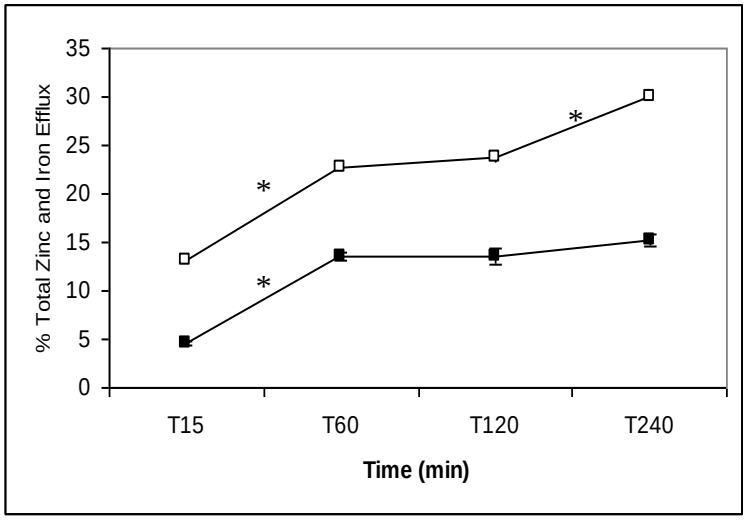

Figure 3.19: % Total of Iron (■) or Zinc (□) Efflux from AML12 cells over 240 minutes. Results are expressed as the amount of zinc or iron released as a percentage of total cellular uptake. Mean ± SE, n = 3 (α = 0.05)**. ***A significant amount of iron and zinc was released from the cell between T_{15} and T_{60} (p = 0.003). The amount of iron released from the cell from T_{60} to T_{240} was negligible as was the amount of zinc released from T_{60} to T_{120}. There was a significant amount of zinc released from T_{120} to T_{240} (p = 0.01).

Subsequent tests were carried out on GFP and GFP/ZnT-1 cells as described in Section 2.4.17. Iron and zinc efflux was measured at 15 min, 30 min, 60 min and 120 min. There was no significant difference in iron efflux between the GFP and GFP/ZnT-1 cells (Figure 3.20a). In contrast zinc efflux was significant between GFP and GFP/ZnT-1 at 60 min (Figure 3.20b).

(a)

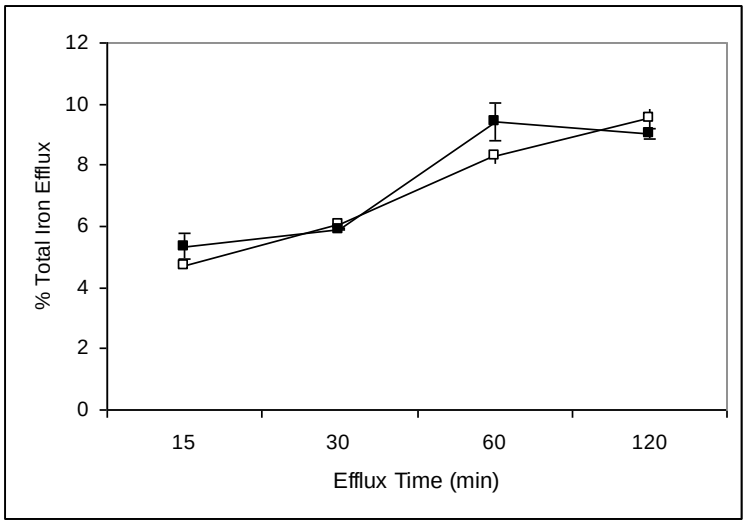

(b)

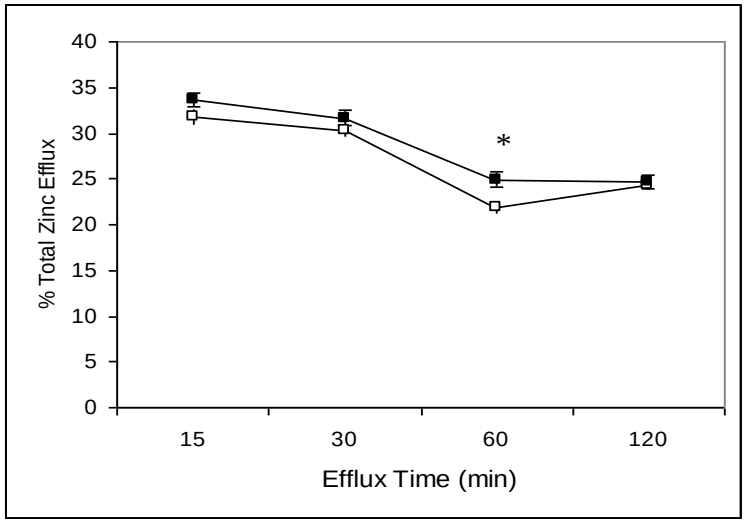

Figure 3.20: % Total of Iron (a) and Zinc (b) efflux from GFP (□) and GFP/ZnT-1 (■) cells over 120 minutes. Results are expressed as the amount of zinc or iron released as a percentage of total cellular uptake. Mean ± SE, n = 3 (α = 0.05). * There was a significant difference in the amount of zinc efflux between GFP and GFP/ZnT-1 cells at 60 minutes ($p < 0.05$). There were no other differences observed in the amount of zinc or iron efflux between GFP and GFP/ZnT-1 cells.

Figure 3.21 shows the internalised fraction of iron and zinc in GFP and GFP/ZnT-1 cells. There was no significant difference observed in internalised iron between GFP and GFP/ZnT-1 cells (Figure 3.21a). However, at 30 minutes there was significantly more zinc internalised in the GFP/ZnT-1 cells compared to the GFP cells (Figure 3.21b). No other notable differences were observed.

(a)

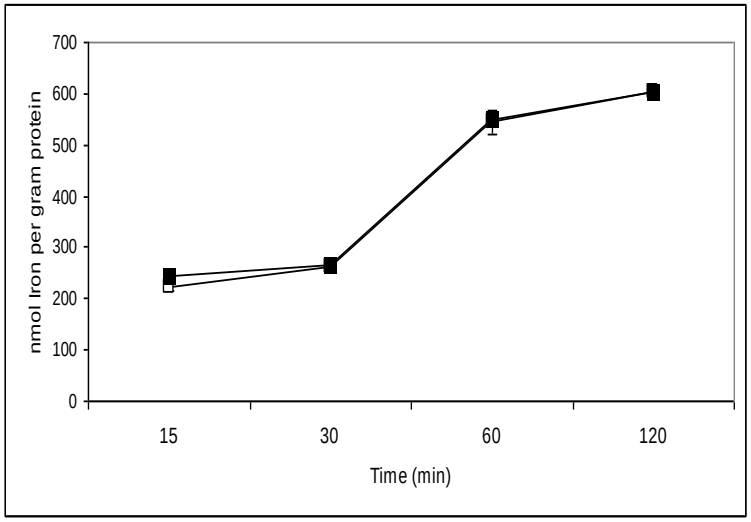

(b)

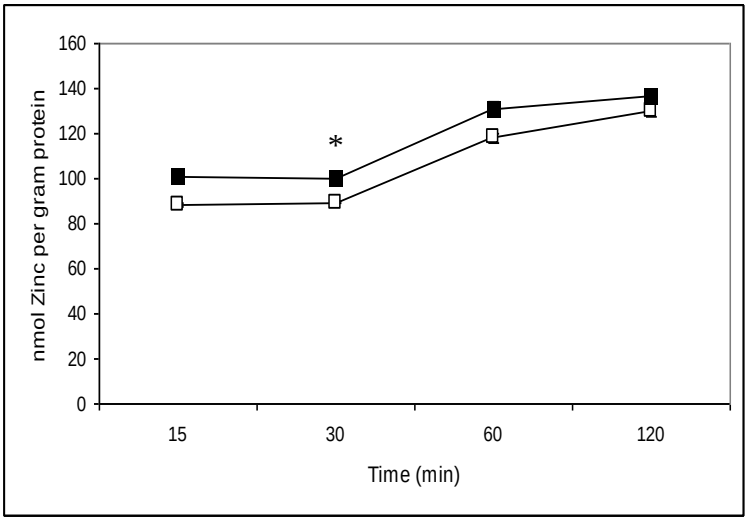

Figure 3.21: nmol of Iron (a) and Zinc (b) internalised in GFP (□) and GFP/ZnT-1 (■) cells. Results are expressed as mean ± SE, n = 3 ($\alpha = 0.05$). * There was a significant difference in the amount of internalised zinc for GFP and GFP/ZnT-1 cells at 30 minutes ($p < 0.05$). There were no other differences observed in the amount of internalised iron or zinc in GFP and GFP/ZnT-1 cells.

3.7 mRNA Expression of Genes in AML12 Cells

RT-PCR was performed on transfected and non-transfected AML12 cells (Section 2.4.5). *ZnT-1* expression was compared with the iron transporters, *Dmt1* and *Zip14*, and the iron exporter *Fpn* to determine whether over-expressing *ZnT-1* had any effect on other transporters.

ZnT-1 (LCI)

ZnT-1 expression was significantly higher in GFP/ZnT-1 and REx/ZnT-1 cells compared to AML12 control cells (Figure 3.22). Expression in GFP-alone cells was no different from control cells. *ZnT-1* expression was increased in REx/ZnT-1 cells compared with AML12 and GFP alone cells, however, *ZnT-1* mRNA expression was significantly higher in GFP/ZnT-1 than in REx/ZnT-1 (Figure 3.22).

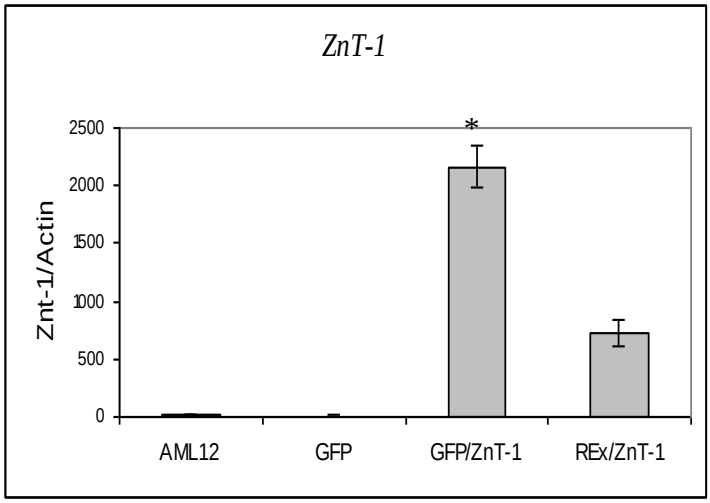

Figure 3.22: *ZnT-1* mRNA expression in AML12, GFP, GFP/ZnT-1 and REx/ZnT-1cells. Results are expressed as mean ± SE, n = 3-6 (α = 0.05). *Significant differences were observed in GFP/ZnT (p = 0.00006) and REx/ZnT-1 cells (p = 0.003).

Fpn, Dmt1 and Zip14

There was no significant difference of *Fpn, Dmt1* and *Zip14* expression between AML12 and GFP, GFP/ZnT-1 and REx/ZnT-1 cells (Figure 3.23; Figure 3.24; Figure 3.25).

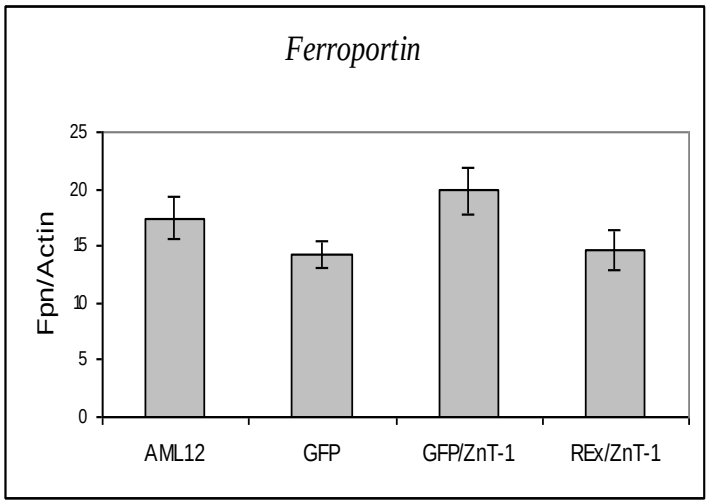

Figure 3.23: *Ferroportin* mRNA expression in AML12, GFP, GFP/ZnT-1 and REx-ZnT-1 cells. Results are expressed as mean ± SEM, n = 3-6 (α = 0.05). There were no significant differences observed (p > 0.05).

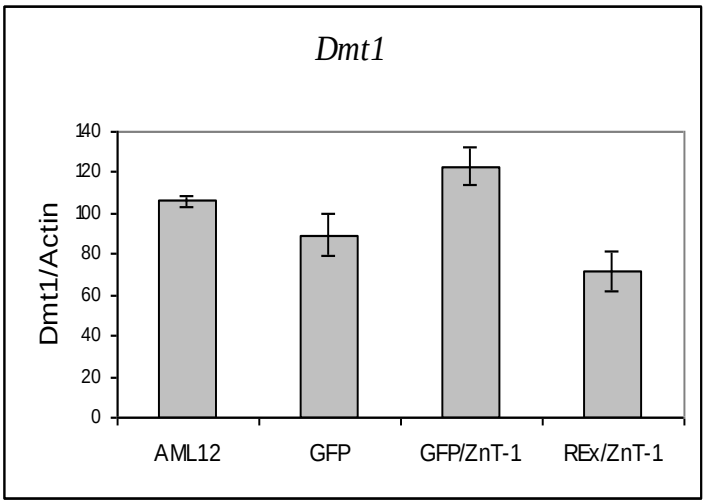

Figure 3.24: *Dmt1* mRNA expression in AML12, GFP, GFP/ZnT-1 and REx/ZnT-1 cells. Results are expressed as mean ± SEM, n = 3-6 (α = 0.05). There were no significant differences observed (p > 0.05).

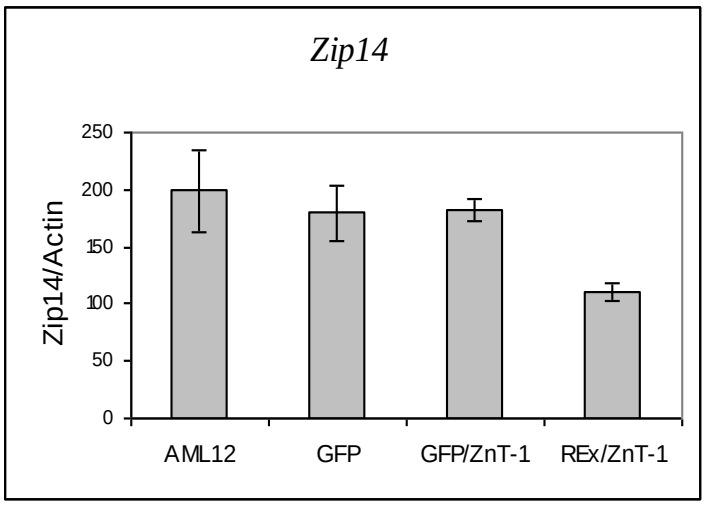

Figure 3.25: *Zip14* mRNA expression in AML12, GFP, GFP/ZnT-1 and REx/ZnT-1 cells. Results are expressed as mean ± SEM, n = 3-6 ($\alpha = 0.05$). There were no significant differences observed ($p > 0.05$).

Chapter 4

Discussion

Introduction

Hereditary haemochromatosis is an autosomal recessive disorder of iron metabolism, characterised by increased iron absorption and progressive iron accumulation particularly in the liver[19]. It has been shown that hepatocytes can acquire iron in two forms; transferrin-bound iron (TBI) and non-transferrin-bound iron (NTBI)[1]. Known transporters of NTBI into the cell include DMT1[84] and ZIP14[32], and FPN is the only transporter known to export iron and evidence suggests that the iron is in the form of ferrous iron[31].

This study involved the characterisation of *ZnT-1*, to determine whether ZNT-1 is involved in the export of iron. mRNA expression was analysed in mouse liver and cells over-expressing ZnT-1. Iron and zinc release was measured in cells over-expressing the ZnT-1 protein.

4.1 Liver mRNA expression

The liver is the main site of iron storage therefore, to analyse the role of ZnT-1 in iron transport, SUI and LUI mRNA expression in mouse liver was examined and compared with the iron metabolism genes *Fpn*, *TfR1* and *Hamp*.

Decreased *ZnT-1* (SUI), *TfR1* and *Hamp* expression was observed in the double mutant mice (Figure 3.6; 3.9; 3.10). In iron deficient livers, there was an increased expression of *ZnT-1* (LUI) and *TfR1* (Figure 3.7; 3.9) and a decrease in *Hamp* expression (Figure 3.10). *Hfe* -/-, *TfR2* mutant and iron loaded mouse livers showed an increase in *Fpn* expression (Figure 3.8). *Hamp* expression was decreased in *Hfe* and *TfR2* mice, there was an increased level of expression in iron loaded mouse models (Figure 3.10).

ZnT-1 expression in wild-type, iron-loaded and TfR2 mice followed a similar trend to previous microarray expression studies. In that unpublished study *ZnT-1* SUI expression was marginally lower in iron-loaded and TfR2 mice compared to wild-type, and *ZnT-1* LUI expression remained unchanged[64].

ZnT-1 is located on the cell membrane and is thought to be involved in zinc efflux[57; 58], and Ohana *et al*. found a reduction of *ZnT-1* expression in cells expressing *ZnT-1* siRNA[85]. Therefore, if ZnT-1 was involved in iron transport, an increase in mRNA expression in iron-loaded liver should have been observed. However, McMahon and Cousins reported an interesting trend in their studies; in response to an acute oral zinc dose, an 8-fold up-regulation of intestinal *ZnT-1* mRNA was observed without a corresponding increase in ZnT-1 protein.

Conversely, liver ZnT-1 protein increased 5-fold without an increase in liver *ZnT-1* mRNA expression suggesting additional factors are involved in ZnT-1 protein regulation[60]. Furthermore, changes in *ZnT-1* expression appear to parallel those of metallothionein 1 (MT-1) which is mediated by MTF-1, suggesting that MTF-1 may also coordinate *ZnT-1* regulation[62].

On that basis, it is reasonable to propose that ZnT-1 is subject to underlying posttranscriptional or posttranslational regulatory factors; however, due to time constraints it was not possible to investigate this further.

The increase in mRNA levels of *TfR1* in iron deficient mice was due to IRP binding to the IRE in the *TfR1* mRNA which prevents mRNA degradation[86].

The increased *Fpn* expression seen in HFE, TfR2 and iron-loaded livers has been reported previously. The function of ferroportin is to export iron from hepatocytes, hence its expression was up-regulated in iron loaded cells and is consistent with previous studies which reported an increase in *Fpn* mRNA in HFE, TfR2 and iron-loaded mice repectively[71; 87; 88]. Ferroportin is regulated in a posttranslational manner by hepcidin. Hepcidin binds to ferroportin and induces its internalisation and degradation thus preventing iron efflux[37]. Hepcidin is regulated by iron status and is secreted from the liver when iron concentration is high to prevent its efflux by ferroportin[89].

The decreased *Hamp* expression observed in HFE, TfR2, iron-deficient and double mutant livers and increased mRNA levels observed in iron-loaded livers is

consistent with previous studies[89; 90; 91; 92; 93]. *Hepcidin* is the key regulator of iron metabolism; in the hepatocyte hepcidin is stimulated with increased iron[89] and down regulated in anemia[90]. In addition, down-regulation of *Hamp* expression has been reported in HFE[91] and TfR2 mutant mouse models[92; 93]. Given that *Hamp* expression was down-regulated in both HFE and TfR2 livers, the decreased *Hamp* expression seen in the double mutant livers is to be expected.

4.2 Cloning *ZnT-1* to produce a GFP fusion protein

Amplifying the *ZnT-1* gene proved to be the most challenging aspect of this study and several PCR reactions were required before a single product of the expected size was obtained. The most troublesome factors were the GC-rich sequences at the 5' end of the gene and the comparatively GC-poor 3' region as well as the high primer melting temperatures (T_M). GC-rich regions generate complex secondary structures which prevent denaturation, annealing and extension during PCR[75] similarly, primers with high T_Ms are susceptible to forming secondary structures[94].

The problem was overcome by using a PCR enhancer and DMSO. PCR enhancers facilitate amplification of problematic templates by increasing primer specificity and allow a wider annealing temperature (T_A) range[95]. DMSO reduces both template and primer T_Ms and relax GC secondary structures[75]. Other factors that required optimisation were $MgCl_2$ concentration and T_A. The first successful amplification contained point mutations and since the product was required for functional studies further PCR reactions were performed using *Pfx50* DNA polymerase which has a fifty times improved fidelity compared with *Taq* DNA

polymerase[80]. Furthermore, a second mutated clone was obtained and the relevance of this will be discussed later.

A single product of the correct size was amplified (Figure 3.11) and successfully cloned to produce pcDNA/GW-N-EmGFP/ZnT-1 and pT-REx/GW/ZnT-1. Sequencing results (Figure 3.13) confirmed the *ZnT-1* gene was cloned and the sequence was free from mutations. Transfection of AML12 cells with pcDNA/GW-N-EmGFP/ZnT-1, pT-REx/GW/ZnT-1 or GFP alone enabled ZnT-1 localisation, qualitative and quantitative analysis as well as functional assays to be performed. AML12 cells transfected with GFP alone controlled for localization of ZnT-1 and REx/ZnT-1 cells were to control for the presence of the GFP tag to validate that functional differences were as a result of *ZnT*-1 expression alone.

The immunoblotting results confirmed the presence of the GFP/ZnT-1 and GFP proteins which were observed at about 80 kDa and 27 kDa, respectively (Figure 3.17). The molecular weight of ZnT-1 protein is 54.5 kDa[96] and the GFP protein is 26.9 kDa[97] therefore, it is to be expected that GFP/ZnT-1 would be observed as 80 kDa. Visualisation of GFP/ZnT-1 cells by fluorescent microscopy is consistent with ZnT-1 being located on the membrane as reported by Palmiter and Findley[57], in contrast to the control cells which showed GFP expression throughout the cell. Furthermore, the punctate staining observed suggests a vesicular localization of the fusion protein (Figure 3.16).

4.3 mRNA Expression of Genes in AML12 cells

It has now been established that DMT1 and ZIP14 are capable of transporting NTBI into cells[32; 84] and FPN is the only transporter known to export iron[31]. *ZnT-1* expression was analysed in untransfected cells and cells transfected with GFP/ZnT-1, GFP alone or REx/ZnT-1 to confirm that cells containing the pcDNA/GW-N-EmGFP/ZnT-1 construct were over-expressing *ZnT-1* and that neither the GFP tag or the plasmid was responsible for functional differences. In addition *ZnT-1* expression was compared with the iron transporters, *Dmt1* and *Zip14*, and the iron exporter *Fpn* to determine whether over-expressing *ZnT-1* had any affect on other transporters.

In cells over-expressing *ZnT-1* there was significantly higher mRNA levels of ZnT-1 than in AML12 cells, GFP cells and REx/ZnT-1 cells. In addition, *ZnT-1* mRNA was significantly higher in REx/ZnT-1 compared to AML12 cells and GFP cells (Figure 3.22). There was no difference in expression of *Fpn, Dmt1* and *Zip14* for GFP, GFP/ZnT-1 or REx/ZnT-1 compared to AML12 cells (Figure 3.23; 3.24; 3.25).

In GFP/ZnT-1 cells, the significantly higher *ZnT-1* expression demonstrated that these cells were over-expressing *ZnT-1* and although REx/ZnT-1 cells were also significantly expressed compared to AML12 cells and cells containing GFP alone, *Znt-1* expression in GFP/ZnT-1 was significantly higher compared to REx/ZnT-1 cells.

If ZnT-1 was involved in iron transport the expression pattern would either mirror that of other transporters, or if its role is to regulate iron influx, as Segal *et al*. suggest occurs with zinc[59], an inverse pattern would be observed. When compared with *Fpn, Dmt1* and *Zip14* expression profiles, there did not appear to be any correlation which might be the reflection of an independent system at work. It is also possible that posttranscriptional regulation inhibited mRNA expression and although this is entirely speculative, *Fpn*, *Dmt1* and *Zip14* have all been shown to be subject to such regulatio[24; 98].

4.4 Iron Uptake and Release

Iron transport was examined by incubating GFP/ZnT-1 and GFP cells with radiolabelled iron to determine whether *ZnT-1* is involved in iron transport. In addition, zinc transport was analysed to validate the efficiency of the assay.

Initial assays were to test whether $^{65}ZnCl_2$ or ^{65}Zn citrate was most efficient for uptake and establish the efficiency of DTPA as a zinc chelator showed that both $^{65}ZnCl_2$ and ^{65}Zn citrate were equally effective at donating zinc to the cells and that DTPA significantly reduced uptake (Figure 3.18). Citrate and DFO are known to be efficient for uptake and release of iron respectively[83], and the use of these in iron assays is standard procedure in this laboratory. Therefore assays were conducted with ^{59}Fe citrate or ^{65}Zn citrate for uptake and DFO or DTPA for release of iron and zinc respectively. In addition, a time course release study established that 90% of the total iron released occurred in the first 60 min and zinc efflux was still occurring at 4 hours (Figure 3.19). Given that the focus of this study was iron transport it was not necessary to test beyond that time point.

Iron and zinc efflux was measured at 15 min, 30 min, 60 min and 120 min in GFP/ZnT-1 and GFP cells. There was no difference in GFP/ZnT-1 iron efflux compared to GFP cells and for zinc efflux the only significant difference observed was at 60 minutes (Figure 3.20). Similarly, with iron and zinc internalization, the only significant difference observed between GFP/ZnT-1 and GFP cells was in zinc at 60 minutes, 130.57 nmol Zn per g protein (+/- 3.65 SE) compared to 118.06 nmol Zn per g protein (+/- 2.15 SE).

Unfortunately, these results remain inconclusive as there was very little difference observed between GFP/ZnT-1 and GFP in zinc uptake and release. *ZnT-1* has been reported to be involved in zinc transport by a number of groups[57; 59; 60; 85; 99] and in contrast to the results observed in this study. Given that zinc uptake and release were measured to validate the assay suggests that the iron uptake and release results are questionable.

However, a number of factors could account for this inconsistency. Segal *et al.*[59] reported no difference in zinc efflux in cells over-expressing *ZnT-1* compared to control cells, however in cells co-expressing the L-type calcium channel (LTCC), a major route for zinc influx, and *ZnT-1*, they observed a 3-fold reduction in zinc influx suggesting that ZnT-1 regulates influx. In addition, Western blot analysis conducted by McMahon and Cousins[60] found intestinal and liver ZnT-1 protein migrated as a 42 and a 36 kDa protein respectively, suggesting post-translational modifications might regulate the steady-state level of ZnT-1 protein. Moreover, given the toxicity of zinc it is reasonable to propose that when subjected to zinc loading, zinc transporters within the cell, compartmentalized the zinc as a

detoxification measure which is consistent with Palmiter *et al*. who reported prolonged exposure of cells expressing *ZnT-2* led to accumulation of zinc in vesicles[51]. Furthermore, Gaither and Eide hypothesised the binding of zinc to metallothionein proteins serve as a detoxification mechanism[46].

4.5 Is there a mutation in *ZnT-1* that produces an aberrant protein?

The SCI was discovered whilst attempting to amplify the *ZnT-1* coding sequence. It was missing 269 nucleotides from its 5' end which translated a 428 amino acid protein. A protein topology prediction revealed a 5 transmembrane protein with an extracellular carboxy terminus which is contrary to the typical ZnT structure[56]. Furthermore, the protein lacked the histidine-rich loop common to most zinc transporters and is thought to act as a metal binding domain[56]. In addition Gaither and Eide reported alterations within the loop affected its metal specificity suggesting it is involved in metal recognition[46]. Unfortunately, due to time constraints it was not possible to investigate this isoform further, however, investigation would be desirable to determine if such an isoform exists and what, if any role it may have in metal transport.

4.6 Future Directions

Due to time constrains there were a number of questions that remain unanswered and require further investigation to establish whether *ZnT-1* is involved in iron transport.

Almost certainly one of the most important issues that need to be established is whether the mutated sequence, namely the SCI of *ZnT-1* is involved in iron transport.

In addition, performing a knockdown and repeating these experiments would be useful to determine whether *ZnT-1* is involved in iron or zinc transport. Additionally, it has been speculated that *Znt-1* is not involved in zinc efflux, but rather regulates its influx. Therefore, establishing whether *ZnT-1* is involved in iron homeostasis by regulating its influx would be valuable.

Moreover, to confirm whether the *Fpn*, *Dmt1* and *Zip14* mRNA expression observed in transfected and untransfected cells was due to mRNA degradation, a time-course study for transfection time could be performed.

Finally, it would be useful to determine whether *ZnT-1* has a hepcidin binding site and is therefore regulated in the same way as ferroportin.

4.7 Conclusion

The liver is the main target of iron deposition, therefore it is reasonable to assume that if *ZnT-1* was involved in iron efflux, it would be highly expressed in the liver in response to iron-loading. However, it is equally logical to suggest that a decrease in *ZnT-1* expression would result in hepatic iron loading characteristic of haemochromatosis. In the present study, the results do not support this hypothesis. Furthermore, cells over-expressing *ZnT-1*, should have released more iron than control cells. Together these results imply that *ZnT-1* is not an iron exporter, in fact, it is even reasonable to question whether it is involved in zinc export. In addition, this study was able to replicate a number of previous studies and as such it can be assumed that the results are reliable.

However, a number of questions remain unanswered and therefore it is not reasonable to definitively state that *ZnT-1* is not an iron exporter. Therefore it is still within the realm of reason that like DMT-1 and ZIP14, it could possibly transport more than one metal.

To date numerous studies have been undertaken in an effort to elucidate the location, function and regulation of zinc transporters as well as their possible role in disease diagnostics, and although a lot has been revealed there is still much to be uncovered. Whether or not that includes the role of *ZnT-1* in iron transport remains to be seen.

References

1. Baker, E., Baker, S. M. and Morgan, E. H. (1998). Characterisation of non-transferrin-bound iron (ferric citrate) uptake by rat hepatocytes in culture. *Biochimica et Biophysica Acta (BBA) - General Subjects* **1380**, 21-30.
2. Melville, J., SCHULTE II, J. & Larson, A. (2004). A molecular study of phylogenetic relationships and evolution of antipredator strategies in Australian Diplodactylus geckos, subgenus Strophurus. *Biological Journal of the Linnean Society* **82**, 123-138.
3. Conrad, M. E., Umbreit, J. N. and Moore, E. G. (1999). Iron Absorption and Transport. *American Journal of the Medical Sciences* **318**, 213-232.
4. Lieu, P. T., Heiskala, M., Peterson, P. A. and Yang, Y. (2001). The roles of iron in health and disease. *Mol Aspects Med* **22**, 1-87.
5. Aisen, P., Enns, C. and Wessling-Resnick, M. (2001). Chemistry and biology of eukaryotic iron metabolism. *International Journal of Biochemistry & Cell Biology* **33**, 940-959.
6. Andrews, N. C. (1999). Disorders of Iron Metabolism. *N Engl J Med* **341**, 1986-1995.
7. Wessling-Resnick, M. (2000). Iron Transport. *Annu. Rev. Nutr.* **20**, 129-151.
8. Andrews, N. C. (2000). Iron Homeostasis: Insights from Genetics and Animal Models. *Nature Genetics* **1**, 208-217.
9. Siah, C. W., Trinder, D. and Olynyk, J. K. (2005). Iron overload. *Clinica Chimica Acta* **358**, 24-36.
10. Douabin, V., Moirand, R., Jouanolle, A., Brissot, P., Le Gall, J., Deugnier, Y. and David, V. (1999). Polymorphisms in the HFE Gene. *Hum Hered* **49**, 21-26.
11. Olynyk, J. K., Cullen, D. J., Aquilla, S., Rossi, E., Summerville, L. and Powell, L. W. (1999). A Population-Based Study of the Clinical Expression of the Hemochromotasis Gene *N Engl J Med* **341**, 718-724.
12. Feder, J. N., Gnirke, A., Thomas, W., Tsuchihashi, Z., Ruddy, D. A., Basava, A., Dormishian, F., Domingo, R., Ellis, M. C., Fullan, A., Hinton, L. M., Jones, N. L., Kimmel, B. E., Kronmal, G. S., Lauer, P., Lee, V. K., Loeb, D. B., Mapa, F. A., McClelland, E., Meyer, N. C., Mintier, G. A., Moeller, N., Moore, T., Morikang, E., Prass, C. E., Quintana, L., Starnes, S. M., Schatzman, R. C., Brunke, K. J., Drayna, D. T., Risch, N. J., Bacon, B. R. and Wolff, R. K. (1996). A novel MHC class I-like gene is mutated in patients with hereditary haemochromatosis. *Nat Genet* **13**, 399-408.
13. Fleming, R. E., and Britton, R.S. (2006). Iron Imports. VI. HFE and regulation of intestinal iron absorption. *Am J Physiol Gastrointest Liver Physiol* **290**, G590-G594.
14. Camaschella, C., Roetto, A., Cali, A., De Gobbi, M., Garozzo, G., Carella, M., Majorano, N., Totaro, A. and Gasparini, P. (2000). The gene TFR2 is mutated in a new type of haemochromatosis mapping to 7q22. *Nature Genetics*, 14-15.
15. Girelli, D., Bozzini, C., Roetto, A., Alberti, F., Daraio, F., Colombari, R., Olivieri, O., Corrocher,R. and Camaschella, C. (2002). Clinical and pathologic findings in hemochromatosis type 3 due to a novel mutation in transferrin receptor 2 gene. *Gastroenterology*, 1295-1302.
16. Deugnier, Y., Brissot, P. and Loreal, O. (2008). Iron and the liver: Update 2008. *J. Hepatol* **48**, S113-S123.

17. Pietrangelo, A. (2004). Non-*HFE* Hemochromatosis. *Hepatology* **39**, 21-29.
18. Zhou, X. Y., Tomatsu, S., Fleming, R. E., Parkkila, S., Waheed, A., Jiang, J., Fei, Y., Brunt, E. M., Ruddy, D. A., Prass, C. E., Schatzman, R. C., O'Neill, R., Britton, R. S., Bacon, B. R. and Sly, W. S. (1998). HFE gene knockout produces mouse model of hereditay hemochromatosis. *Proc Natl Acad Sci USA* **95**, 2492-2497.
19. Fleming, R. E., Ahmann, J. R., Migas, M. C., Waheed, A., Koeffler, H. P., Kawabata, H., Britton, R. S., Bacon, B. R. and Sly, W. S. (2002). Targeted mutagenesis of the murine transferrin receptor-2 gene produces hemochromatosis. *Proc Natl Acad Sci USA* **99**, 10653-10658.
20. Fleming, R., Britton, R., Migas, M., Rozier, M., Waheed, A. and Sly, W. (2009). *The Third Congress of the International BioIron Society and 8th International Symposium on Microbial Iron Transport, Storage and Metabolism, Porto, Portugal*.
21. Subramaniam, S., Summerville, L., Crampton, E., Frazer, D., Anderson, G. and Wallace, D. (2009). *The Third Congress of the International BioIron Society and 8th International Symposium on Microbial Iron Transport, Storage and Metabolism, Porto, Portugal*.
22. Delima, R., Chua, A., Herbison, C., Graham, R. M., Olynyk, J. and Trinder, D. (2009). *The Third Congress of the International BioIron Society and 8th International Symposium on Microbial Iron Transport, Storage and Metabolism, Porto, Portugal*.
23. Ponka, P. (2002). Rare cases of hereditary iron overload. *Seminars in Hematology* **39**, 249-262.
24. Chung, J., and Wessling-Resnick, M. (2003). Molecular mechanisms and regulation of iron transport. *Crit Rev Clin Lab Sci* **40**, 151-182.
25. Miret, S., Simpson, R. J. and McKie, A. T. (2003). Physiology and Molecular Biology of Dietary Iron Absorption. *Annu. Rev. Nutr.* **23**, 283-301.
26. Morgan, E. H., and Oates, P. S. (2002). Mechanisms and Regulation of Intestinal Iron Absorption. *Blood Cells, Molecules, & Diseases* **29**, 384-399.
27. Fleming, R. E., and Bacon, B. R. (2005). Orchestration of Iron Homeostasis. *N Engl J Med* **352**, 1741-1744.
28. Trinder, D., Fox, C., Vautier, G. and Olynyk, J. K. (2002). Molecular pathogenesis of iron overload. *Gut* **51**, 290-295.
29. Chua, A. C. G., Graham, R. M., Trinder, D. and Olynyk J. K. (2007). The Regulation of Cellular Iron Metabolism. *Crit Rev Clin Lab Sci* **44**, 413-459.
30. Sharma, N., Butterworth, J., Cooper, B. T., Tselepis, C. and Iqbal, T. H. (2005). The Emerging Role of the Liver in Iron Metabolism. *Am J Gastroenterol* **100**, 201-206.
31. Graham, R. M., Chua, A. C. G., Herbison, C. E., Olynyk, J. K. and Trinder, D. (2007). Liver iron transport *World J Gastroenterol* **13**, 4725-4736.
32. Luizzi, J. P., Aydemir, F., Nam, H., Knutson, M. D. and Cousins, R. J. (2006). Zip14 (Slc39a14) mediates non-transferrin-bound iron uptake into cells. *Proc Natl Acad Sci USA* **103**, 13612-13617.

33. Ponka, P., and Lok, C. N. (1999). The transferrin receptor: role in health and disease. *Int J Biochem & Cell Biol* **31**, 1111-1137.
34. Philpott, C. C. (2002). Molecular Aspects of Iron Absorption: Insights Into the role of HFE in Hemochromatosis. *Hepatology* **35**, 993-1001.
35. Barisani, D., and Conte, D. (2002). Transferrin Receptor 1 (TfR1) and Putative Stimulaor of Fe Transport (SFT) Expression in Iron Deficiency and Overload: An Overview. *Blood Cells, Molecules, & Diseases* **29**, 498-505.
36. Niles, B. J., Clegg, M. S., Hanna, L. A., Chou, S. S., Momma, T. Y., Hong, H. and Keen, C. L. (2008). Zinc Deficiency-induced Iron Accumulation, a Consequence of Alterations in Iron Regulatory Protein-binding Activity, Iron Transporters, and Iron Storage Proteins. *J. Biol. Chem* **283**, 5168-5177.
37. Nemeth, E., Tuttle, M. S., Powelson, J., Vaughan, M. B., Donovan, A., McVey Ward, D., Ganz, T. and Kaplan, J. (2004). Hepcidin Regulates Cellular Iron Efflux by binding to Ferroportin and Inducing its Internalization. *Science* **306**, 2090-2093.
38. Berg, J. M., and Shi, Y. (1996). The Galvanization of Biology: A Growing Appreciation for the roles of Zinc. *Science* **271**, 1081-1085.
39. Tapiero, H., and Tew, K. D. (2003). Trace elements in human physiology and pathology: zinc and metallothioneins. *Biomedicine & Pharmacotherapy* **57**, 399-411.
40. Keilin, D., and Mann, T. (1940). Carbonic Anhydrase. Purification and Nature of the Enzyme. J. Biochem. *J. Biochem* **34**, 1163-1176.
41. Andreini, C., Banci, L., Bertini, I. and Rosato, A. (2006). Counting the Zinc Proteins Encoded in the Human Genome. *J. Proteome Res* **5**, 196-201.
42. Vallee, B. L., and Auld, D. S. (1990). Zinc coordination, function, and structure of zinc enzymes and other proteins. *Biochem* **29**, 5647-5659.
43. Hershfinkel, M., Silverman, W. F. and Sekler, I. (2007). The Zinc Sensing Receptor, a Link Between Zinc and Cell Signalling. *Mol. Med.* **13**, 331-336.
44. MacDonald, R. S. (2000). The Role of Zinc in Growth and Cell Proliferation. *J. Nutr.*, 1500S-1508S.
45. Hershfinkel, M., Moran. A., Grossman, N. and Sekler, I. (2001). A zinc-sensing receptor triggers the release of intracellular Ca2+ and regulates ion transport. *Proc Natl Acad Sci USA* **98**, 11749-11754.
46. Gaither, L. A., and Eide, D. J. (2001). Eukayotic zinc transporters and their regulation. *Biometals* **14**, 251-270.
47. Kambe, T., Yamaguchi-Iwai, Y., Sasaki, R. and Nagao, M. (2004). Overview of mammalian zinc transporters. *Cell. Mol. Life Sci* **61**, 49-68.
48. Krebs, N. F. (2000). Overview of Zinc Absorption and Excretion in the Human Gastrointestinal Tract. *J. Nutr.* **130**, 1374S-1377S.
49. Reyes, J. G. (1996). Zinc transport in mammalian cells. *J. Physiol.* **270**.
50. Coyle, P., Philcox, J. C., Carey, L. C. and Rofe, A. M. (2002). Metallothionein: the multipurpose protein. *Cell Mol. Life Sci.* **59**, 627-647.
51. Palmiter, R. D., Cole, T. B. and Findley, S. D. (1996). ZnT-2, a mammalian protein that confers resistance to zinc by facilitating vesicular sequestration. *Embo J.* **15**, 1784-1791.

52. Eide, D. J. (2006). Zinc Transporters and the cellular trafficking of zinc. *Biochimica et Biophysica Acta* **1763**, 711-722.
53. Hediger, M. A., Romero, M. F., Peng, J-B., Rolfs, A., Takanaga, H. and Bruford, E. A. (2004). The ABCs of solute carriers: physiological, pathological and therapeutic implications of human membrane transport proteins. *Eur. J. Physiol* **447**, 465-468.
54. Luizzi, J. P., and Cousins, R. J. (2004). Mammalian Zinc Transporters. *Annu Rev. Nutr*. **24**, 151-172.
55. Cousins, R. J., Luizzi, J. P. and Lichten, L. A. (2006). Mammalian Zinc Transport, Trafficking, and Signals. *J. Biol. Chem* **281**, 24085-24089.
56. Harris, E. D. (2002). Cellular Transporters for Zinc. *Nutrition Rev.* **60**, 121-124.
57. Palmiter, R. D., and Findley, S. D. (1995). Cloning and functional characterization of a mammalian zinc transporter that confers resistance to zinc. *Embo J.* **14**, 639-649.
58. Palmiter, R. D., and Huang, L. (2004). Efflux and compartmentalization of zinc by members of the SLC30 family of solute carriers. *Eur. J. Physiol* **447**, 744-751.
59. Segal, D., Ohana, E., Besser, L., Hershfinkel, M., Moran, A. and Sekler, I. (2004). A role for ZnT-1 in regulating cellular cation influx. *BBRC* **323**, 1145-1150.
60. McMahon, R. J., and Cousins, R. J. (1998). Regulation of the zinc transporter ZnT-1 by dietary zinc. *Proc Natl Acad Sci USA* **95**, 4841-4846.
61. Sekler, I., Sensi, S., Hershfinkel., M. and Silverman, W. F. (2007). Mechanism and Regulation of Cellular Zinc Transport. *Molecular Medicine* **13**, 337-343.
62. Langmade, S. J., Ravindra, R., Daniels, P. J. and Andrews, G. K. (2000). The Transcription Factor MTF-1 Mediates Metal Regulation of the Mouse ZnT1 Gene. *J. Biol. Chem* **275**, 34803-34809.
63. Yu, Y. Y., Kirschke, C. P. and Huang, L. (2007). Immunohistochemical Analysis of ZnT1, 4, 5, 6, and 7 in the Mouse Gastrointestinal Tract. *J Histochem Cytochem* **55**, 223-234.
64. Graham, R. M. (2007). Microarray of wild type, iron-loaded and TfR2 mutant mouse liver, *Personal communication of unpublished data*.
65. Primer3 v. 0.4.0 (2007), URL: http://frodo.wi.mit.edu/primer3/, Accessed 13/08/2007.
66. Kalinowski, S., Wagner, A. & Taper, M. (2006). ML-Relate: a computer program for maximum likelihood estimation of relatedness and relationship. *Molecular Ecology Notes* **6**, 576-579.
67. Inoue, H., Nojima, H. and Okayama, H. (1990). High efficiency transformation of *Escherichia coli* with plasmids. *Gene* **96**, 23-28.
68. Chua, A. C. G., Herbison, C. E., Drake, S. F., Graham, R. M., Olynyk, J. K. and Trinder, D. (2008). The role of Hfe in transferrin-bound iron uptake by hepatocytes. *Hepatology* **47**, 1737-44.
69. Nicolas, G., Bennoun, M., Devaux, I., Beaumont, C., Grandchamp, B., Kahn, A. and Vaulont, S. (2001). Lack of hepcidin gene expression and severe tissue iron overload in upstream stimulatory factor 2 (USF2) knockout mice. *Proc Natl Acad Sci USA* **98**, 8780-8785.
70. Dupic, F., Fruchon, S., Bensaid, M., Borot, N., Radosavljevic, M., Loreal, O., Brissot, P., Gilfillan, S., Bahram, S., Coppin, H. and Roth M. P.

(2002). Inactivation of the hemochromatosis gene differentially regulates duodenal expression of iron-related mRNAs between mouse strains. *Gastroenterology* **122**, 745-51.

71. Drake, S. F., Morgan, E. H., Herbison, C. E., Delima, R., Graham, R. M., Chua, A. C. G., Leedman, P. J., Fleming, R. E., Bacon, B R., Olynyk, J. K. and Trinder, D. (2006). Iron absorption and hepatic iron uptake are increased in a transferrin receptor 2 (Y245X) mutant mouse of hemochromatosis type 3. *Am J Physiol Gastrointest Liver Physiol* **292**, 323-328.
72. Girijashanker, K., He, L., Soleimani, M., Reed, J. M., Li, H., Liu, Z., Wang, B., Dalton, T. P. and Nebert, D. W. (2008). Slc39a14 Gene Encodes ZIP14, A Metal/Bicarbonate Symporter: Similarities to the ZIP8 Transporter. *Mol Pharmacol* **73**, 1413-1423.
73. Ralser, M., Querfurth, R., Warnatz, H-J., Lehrach, H., Yaspo, M-L. and Krobitsch, S. (2006). An efficient and economic enhancer mix for PCR. *BBRC* **347**, 747-751.
74. Frackman, S., Kobs, G., Simpson, D. and Storts, D. (1998). Betaine and DMSO: Enhancing Agents for PCR. In *Promega Notes*, Vol. 65, pp. 27.
75. Sahdev, S., Saini, S., Tiwari, P., Saxena, S. and Saini, K. S. (2007). Amplification of GC-rich genes by following a combinatioin strategy of primer design, enhancers and modified PCR cycle conditions. *Mol. Cell Probes* **21**, 303-307.
76. Invitrogen. (2003). Gateway® Technology: A universal technology to clone DNA sequences for functional analysis and expression in multiple systems, Version E.
77. CodonCode Corporation, CodonCode Aligner v.20.6 (2006-2007), URL: http://www.codoncode.com/aligner/, Accessed 30/01/2008
78. Informagen Inc., Sequence Analysis v. 1.6.0 (2006), URL: http://www.informagen.com/SA/, Accessed 15/04/2008
79. Ririe, K. M., Rasmussen, R. P. and Wittwer, C. T. (1997). Product differentiation by Analysis of DNA Melting Curves during the Polymerase Chain Reaction. *Anal. Biochem* **245**, 154-160.
80. Invitrogen. (2006). *Pfx50* DNA Polymerase Specification Sheet, pp. 1-4.
81. Geneious v. 3.7.1 (2008), URL: http://www.geneious.com/, Accessed: 07/07/2008.
82. NCBI, Accession No. NP_033605.1, Zinc transporter [Mus musculus]URL: http://www.ncbi.nlm.nih.gov/protein/6678017, Accessed: 29/08/2008.
83. Roy, C. N. (1999). The hereditary hemochromatosis protein, HFE, specifically regulates transferrin-mediated iron uptake in HeLa cells. *J. Biol. Chem.* **274**, 9022-9028.
84. Chua, A. C. G., Olynyk, J. K., Leedman, P. J. and Trinder, D. (2004). Nontransferrin-bound iron uptake by hepatocytes is increased in the *Hfe* knockout mouse model of hereditary hemochromatosis. *Blood* **104**, 1519-1525.
85. Ohana, E., Sekler, I., Kaisman, T., Kahn, N., Cove, J., Silverman, W. F., Amsterdam, A. and Hershfinkel, M. (2006). Silencing of ZnT-1 expression enhances heavy metal influx and toxicity. *J. Mol Med* **84**, 753-763.
86. Casey, J. L., Koeller, D. M., Ramin, V. C., Klausner, R. D. and Harford, J. B. (1989). Iron regulation of transferrin receptor mRNA levels requires

iron-responsive elements and a rapid turnover determinant in the 3' untranslated region of the mRNA. *Embo J.* **8**, 3693-3699.

87. Gleeson, F., Ryan, E., Barrett, S., Russell, J. and Crowe, J. (2006). Hepatic iron metabolism gene expression profiles in HFE associated Hereditary Hemochromatosis. *Blood Cells, Molecules, & Diseases* **38**, 37-44.
88. Aydemir, F., Jenkitkasemwong, S., Gulec, S. and Knutson, M. D. (2009). Iron Loading Increases Ferroportin Heterogeneous Nuclear RNA and mRNA Levels in Murine J774 Macrophages. *J. Nutr*. **139**, 434-438.
89. Rossi, E. (2005). Hepcidin - the Iron Regulatory Hormone. *Clin Biochem Rev* **26**, 47-49.
90. Nicolas, G., Bennoun, M., Porteu, A., Mativet, S., Beaumont, C., Grandchamp, B., Sirito, M., Sawadogo, M., Kahn, A. and Vaulont, S. (2002). Severe iron deficiency anemia in transgenic mice expressing liver hepcidin. *Proc Natl Acad Sci USA* **99**, 4596-4601.
91. Bridle, K. R., Frazer, D. M., Wilkins, S. J., Dixon, J. L., Purdie, D. M., Crawford, D. H. G., Subramaniam, N., Powell, L. W., Anderson, G. J. and Ramm, G. A. (2003). Disrupted hepcidin regulation in *HFE*-associated haemochromatosis and the liver as a regulator of body iron homeostasis. *Lancet* **361**, 669-673.
92. Nemeth, E., Roetto, A., Garozzo, G., Ganz, T. and Camaschella, C. (2005). Hepcidin is decreased in TFR2 hemochromatosis. *Blood* **105**, 1803-1806.
93. Kawabata, H., Fleming, R. E., Gui, D., Moon, S. Y., Saitoh, T., O'Kelly, J., Umehara, Y., Wano, Y., Said, J. W. and Koeffler, P.H. (2004). Expression of hepcidin is down-regulated in TfR2 mutant mice manifesting a phenotype of hereditary hemochromatosis. *Blood* **105**, 376-381.
94. Frey, U. H., Bachmann, H. S., Peters, J. and Siffert, W. (2008). PCR-amplification of GC-rich regions: 'slowdown PCR'. *Nature Protocols* **3**, 1312-1317.
95. Invitrogen. (2008). PCRx Enhancer System Specification Sheet, pp. 1-4.
96. NCBI. Solute carrier family 30 (zinc transporter), member 1 [Mus musculus] NP_033605.1.
97. Chalfie, M., Euskirchen, G., Ward, W. W. and Prasher D. C. (1994). Green Fluorescent protein as a marker for gene expression. *Science* **11**, 802-805.
98. Gao, J., Zhao, N., Knutson, M. D. & Enns, C. A. (2008). The hereditary hemochromatosis protein, HFE, inhibits iron uptake via down-regulation of Zip14 in HepG2 cells. *Journal of Biological Chemistry* **283**, 21462.
99. Overbeck, S., Uciechowski, P., Ackland, L., Ford, D. and Rink, L. (2008). Intracellular zinc homeostasis in leukocyte subsets is regulated by different expression of zinc exporters ZnT-1 to ZnT-9. *J. Leukoc. Biol* **83**, 368-380.